The SNARE protein, syntaxin1a, plays an essential role in biphasic exocytosis of the incretin hormone, glucagon-like peptide-1

Journal:	*Diabetes*
Manuscript ID	DB16-1403.R1
Manuscript Type:	Original Article: Metabolism
Date Submitted by the Author:	n/a
Complete List of Authors:	Wheeler, Sarah; University of Toronto, Dept of Physiology Stacey, Holly; University of Toronto, Dept of Physiology Nahaei, Yasaman; University of Toronto, Dept of Physiology Hale, Stephen; University of Toronto, Dept of Physiology Hardy, Alexandre; University of Toronto Reimann, Frank; University of Cambridge, Clinical Biochemistry Gribble, Fiona; University of Cambridge, CCambridge Institute for Medical Research and MRC Metabolic Diseases Unit Larraufie, Pierre; University of Cambridge, CCambridge Institute for Medical Research and MRC Metabolic Diseases Unit Gaisano, Herbert; University of Toronto, Medicine Brubaker, Patricia; University of Toronto, Dept of Physiology; University of Toronto, Dept of Medicine
Note: The following files were submitted by the author for peer review, but cannot be converted to PDF. You must view these files (e.g. movies) online.	
Supplemental Video 1 - avi.avi Supplemental Video 1 - mp4.mp4 Supplemental Video 2 - avi.avi Supplemental Video 2 - mp4.mp4 Supplemental Video 3 - avi.avi Supplemental Video 3 - avi.mp4	

The SNARE protein, syntaxin1a, plays an essential role in biphasic exocytosis of the incretin hormone, glucagon-like peptide-1

Sarah E. Wheeler[1], Holly M. Stacey[1], Yasaman Nahaei[1], Stephen J. Hale[1], Alexandre B. Hardy[2], Frank Reimann[3], Fiona M. Gribble[3], Pierre Larraufie[3], Herbert Y. Gaisano[1,4] and Patricia L. Brubaker[1,4]

Departments of [1]Physiology and [4]Medicine, University of Toronto, Toronto, ON M5S 1A8, Canada; [2]3D CFI Centre, University of Toronto, Toronto, ON M5S 1A8, Canada; and [3]Wellcome Trust-MRC Institute of Metabolic Science, Metabolic Research Laboratories, University of Cambridge, Addenbrooke's Hospital, Box 289, Hills Rd, Cambridge, CB2 0QQ, United Kingdom.

Running title: Role of syntaxin-1a in biphasic GLP-1 secretion

Corresponding Author: Dr. P.L. Brubaker, Rm 3366 Medical Sciences Building, University of Toronto, 1 King's College Circle, Toronto, ON M5S 1A8, Canada. Tel: 1-416-978-2593; email p.brubaker@utoronto.ca

Metrics: Abstract, 200 words; Text, 4,497 words; References, 57; Figures, 6; Supplementary Figures, 7; Supplementary videos, 6; Supplementary tables, 3.

Abstract

Exocytosis of the hormone, glucagon-like peptide-1 (GLP-1), by the intestinal L-cell is essential for the incretin effect after nutrient ingestion, and is critical for the actions of dipeptidylpeptidase IV inhibitors that enhance GLP-1 levels in patients with type 2 diabetes. 2-Photon microscopy revealed that exocytosis of GLP-1 is biphasic, with a 1st peak at 1-6min and a 2nd peak at 7-12min after stimulation with forskolin. Approximately 75% of the exocytotic events were represented by compound granule fusion, and the remainder were accounted for by full fusion of single granules, under basal and stimulated conditions. The core SNARE protein, syntaxin-1a (syn1a), was expressed by murine ileal L-cells. At the single L-cell level, 1st phase forskolin-induced exocytosis was reduced to basal ($p<0.05$) and 2nd phase exocytosis was abolished ($p<0.05$) by syn1a knockout. L-cells from intestinal-epithelial syn1a-deficient mice demonstrated a 63% reduction in forskolin-induced GLP-1 release in vitro ($p<0.001$), and a 23% reduction in oral glucose-stimulated GLP-1 secretion ($p<0.05$) in association with impairments in glucose-stimulated insulin release (by 60%, $p<0.01$) and glucose tolerance (by 20%, $p<0.01$). Our findings therefore identify an exquisite mechanism of metered secretory output that precisely regulates release of the incretin hormone, GLP-1 and, hence, insulin secretion following a meal.

Keywords: 2-photon microscopy, exocytosis, GIP, GLP-1, GLP-2, intestine, knockout, OGTT, oxyntomodulin, primary cells, proglucagon-Venus, secretion, villin-cre

Introduction

The incretin hormone, glucagon-like peptide-1 (GLP-1), plays an essential role in the maintenance of normoglycemia, through enhancement of glucose-dependent insulin secretion and suppression of glucagon release, gastric emptying and appetite (1, 2). As a consequence of these beneficial actions, GLP-1 receptor agonists are now widely-utilized to treat patients with type 2 diabetes (T2D) and obesity. In contrast to the actions of GLP-1-derivative drugs, therapeutic dipeptidylpeptidase IV (DPP IV) inhibitors prevent the degradation of endogenously-secreted GLP-1, as well as of the other incretin hormone, glucose-dependent insulinotropic peptide (GIP) (3, 4). The possibility of utilizing GLP-1 secretagogues, alone or in combination with DPP IV inhibition, has therefore engendered considerable interest as a new approach to incretin therapy (5-7).

Hormone secretion by the intestinal L-cell which includes, not only GLP-1 but also the related peptides, GLP-2 and oxyntomodulin, demonstrates two peaks of release following nutrient ingestion (8, 9). Rodent studies have demonstrated that part of the early peak of GLP-1 secretion is mediated indirectly, through vagal pathways originating in the duodenum that activate muscarinic receptors on the distal L-cell (10-12). In contrast, the later peak of GLP-1 release is initiated by direct contact of luminal nutrients with the L-cell, resulting in transporter- and ion channel-mediated depolarization, as well as activation of multiple G protein-coupled receptors (13-16). Many of these receptors are expressed not only by the intestinal L-cell, but also by the pancreatic β-cell (17), consistent with the coordinated release of GLP-1 and insulin in vivo. However, in contrast to the β-cell, for which the signaling pathways regulating insulin secretion are well-established (18), much less is known about the intestinal L-cell.

Glucose-mediated depolarization of the β-cell opens voltage-gated calcium channels, thereby activating the calcium-sensor, synaptotagmin-7 (19). This relieves the clamping action of synaptogamin-7 on the SNARE fusion machinery, which consists of the vesicle SNARE protein, VAMP, and the plasma membrane SNAREs, syntaxin (syn) and SNAP23/25 (20), thus permitting insulin exocytosis. Although the β-cell expresses several SNARE isoforms, VAMP2 and syn1a are most important for 1st phase glucose-stimulated insulin secretion (GSIS), with VAMP8 and syn3/4 contributing to both 1st and 2nd phase release (21-23). The SNARE proteins also mediate several different types of exocytotic events in the β-cell. Thus, predocked secretory granules (SGs) contribute predominantly to 1st phase secretion, whereas newcomer granules recruited from an intracellular reserve pool account for some of 1st phase and practically all of 2nd phase insulin exocytosis (24). Furthermore, these SGs also undergo temporally and physically distinct types of fusion with the plasma membrane, termed full, sequential, compound and kiss-and-run (24-29).

While one study has demonstrated a role for synaptotagmin-7 in GLP-1 secretion (30), little is known about the role of the core SNARE proteins in the L-cell. We have reported that the murine GLUTag L-cell line expresses multiple isoforms of VAMP and syn, as well as SNAP25 (31). VAMP2 was demonstrated to play an important role in GLP-1 secretion by these cells, and was also found to be expressed in primary mouse intestinal L-cells. Furthermore, VAMP2 co-immunoprecipitates with syn1a and SNAP25 in the GLUTag cells, suggesting these SNARE proteins form a functional exocytotic complex in the L-cell. Given the current interest in therapeutic approaches to enhance release of GLP-1 into the circulation (5-7), we have now utilized novel knockout mouse models in vivo and ex vivo, in combination with single-cell visualization of exocytosis, to interrogate GLP-1 release by the primary intestinal L-cell. We

show that GLP-1 release is biphasic, as mediated primarily by multi-granular (i.e. compound) fusion under both basal and stimulated conditions, and that the SNARE protein, syn1a, plays an essential role in the exocytosis of GLP-1. These findings identify novel regulatory mechanisms that underlie secretion of the incretin hormone, GLP-1, and have implications to the development of GLP-1 secretagogues for therapeutic use in the treatment of T2D and obesity.

Methods

Animals Male C57Bl/6 mice (7-12 wk) were from Charles River. Female syn1a$^{fl/fl}$ (32) were crossed with male villin-creER$^{T2+/0}$ (B6-Tg(Vil-cre/ERT2)23Syr) (33, 34) mice and the resultant tamoxifen-inducible intestinal-epithelial syn1a$^{fl/fl}$;villin-creER$^{T2+/0}$ (IE-syn1a KO) animals were crossed with proglucagon (*Gcg*)-Venus mice (35) to generate Venus-IE-syn1a KO animals (see Table S1 for primers). Age- (7-12 wk) and sex-matched male and female littermates were studied, and controls included: vehicle- and tamoxifen (1 mg/100 µl sunflower oil, ip for 5 d)-treated syn1a$^{fl/fl}$, villin-creER$^{T2+/0}$, syn1a$^{fl/-}$;villin-creER$^{T2+/0}$ and syn1a$^{fl/-}$;villin-creER$^{T2+/0}$;*Gcg*-Venus mice, as well as vehicle-treated syn1a$^{fl/fl}$;villin-creER$^{T2+/0}$ and syn1a$^{fl/fl}$;villin-creER$^{T2+/0}$;*Gcg*-Venus animals, as appropriate for the KO model being studied. Two-three days after induction, mice were fasted overnight followed by an oral or intraperitoneal glucose tolerance test (OGTT: 5g/kg glucose; as previously shown to optimize GLP-1 release in mice (36); and IPGTT: 3 g/kg glucose, as determined in pilot studies to match the glycemic response observed in the OGTT, data not shown) and tail-vein blood collection. Glycemia was determined using a glucose meter (OneTouch, LifeScan), and plasma total GLP-1 (Mesoscale Discovery), total GIP (Millipore) and insulin (Crystal Chem) by kit-assay, as reported (37). Due to their high concentration of L-cells (38), ileal segments were collected for primary culture and analyses. All animal protocols were approved by the Animal Care Committee of the University of Toronto.

Adult mouse ileal crypt (AMIC) cultures Isolated crypts from 10-cm mouse ileum were plated overnight, as reported (35). Two-hr secretion assays were followed by ELISA (Millipore) for active GLP-1 levels in media and cells, as reported (12, 35). Secretion was calculated as the

percent of total culture content that was detected in the media. Experiments were conducted in quadruplicate wells to make n=1 per mouse.

2-Photon microscopy was performed on AMIC cultures perfused at 2 ml/min and 30 ^{o}C. Sulforhodamine-B (0.8 mM) (25) was added 2-3 min prior to visualization using a Nikon A1R multi-photon microscope, for up to 3 min (basal) followed by 12 min with 50 μM forskolin. L-cells were identified by Venus (YFP) fluorescence, and the cell membrane was defined by the extracellular localization of sulforhodamine-B. Data were analysed with NIS-Elements software (Nikon). Focal events that occurred over ≤10 sec were classified as full fusion, whereas events of longer duration were considered to be compound fusion.

Morphometric and immunometric analyses Crypt-villus height was measured in hematoxylin & eosin-stained ileal sections in a minimum of 20 well-oriented axes per mouse. Ileal sections and AMIC cultures were stained for syn1a and GLP-1 (see Table S2 for antibodies), followed by visualization using a Zeiss deconvolution microscope and analysis of fluorescence intensity using ImageJ# (39). Negative controls omitted the primary antisera.

Molecular analyses Ileal Venus^{+} and Venus^{-} cells were collected from female *Gcg*-Venus mice (n=3) by fluorescence-activated cell sorting. Barcode-ligation and end repair were achieved using the Ovation Rapid DR Multiplex System 1–96 (NuGEN). Combined barcoded libraries underwent SE50 sequencing using an Illumina HiSeq 2500 system (Genomics Core Facility, Cancer Research UK Cambridge Institute). Sequence reads were demultiplexed using the Casava pipeline (Illumina) and aligned to the mouse genome (GRCm38) using Tophat-v2.1.0 (http://ccb.jhu.edu/software/tophat/index.shtml). Differential gene expression was determined using Cufflinks-v2.2.1 (http://cole-trapnell-lab.github.io/cufflinks/), as reported (35).

Total RNA from ileal mucosal scrapes and AMIC cultures was reverse-transcribed and analyzed by PCR with primer/probe sets from Applied Biosystems (Table S3). Histone 3A was used as the internal control for analysis by the ΔΔCt method.

Adenovirus studies: Syn1a$^{fl/fl}$ mice were anesthetized, laparotomized and 0.75 ml of 0.9-1.8x10^{8} infection units/ml Adenovirus-RFP-improved cre-recombinase (Adv-iCre) or Adv-RFP (control; Vector Biolabs) was injected into the distal ileal lumen. Animals recovered for 2d and were then re-laparotomized and 0.75 ml oleoylethanolamide (OEA; 15 μM) was injected into the ileum followed by sampling for analysis of glycemia, plasma hormone levels and ileal gene expression, as above.

AMIC cultures were infected with 2.4x10^{7} IFU/ml Adv-iCre or Adv-RFP for 48 hr, followed by a 2 hr GLP-1 secretion assay and analysis by ELISA and qRT-PCR, as above.

Statistical Analyses Data are shown as mean ± SEM. Statistical differences were determined by Student's t test or 1- or 2-way ANOVA followed by Student's t test or Tukey multiple comparison test, as appropriate.

Results

Immunostaining of the ileum from normal mice revealed expression of syn1a in GLP-1-expressing cells, as well as in other cells in the crypt and scattered through the villous epithelium (Figure 1A). We also examined co-localization of GLP-1 and syn1a in AMIC cultures, a valuable ex vivo model for the study of GLP-1 secretion by primary L-cells (35) (Figure 1B). Importantly, of the 1.1 ± 0.1% of all AMIC cells that were GLP-1-positive (n=1670-5095 cells each in 6 independent cultures), 100% were found to co-express syn1a. Confirming specificity of the syn1a staining, AMIC cultures generated from intestinal-epithelial syn1a knockout (IE-syn1a KO) mice demonstrated a significant loss of syn1a staining in the L-cells ($p<0.001$) as well as more globally in other, unidentified crypt cells (Figure 1C-D).

GLP-1 secretion by AMIC cultures from normal mice was increased to 2.3-fold of control ($p<0.01$) in response to treatment with forskolin plus 3-isobutyl-1-methylxanthine (IBMX), without any change in GLP-1 synthesis (Figures 1E-F). Similarly, treatment with the physiological secretagogues, GIP (Figure 1G) and the GPR119 agonist, oleoylethanolamide (OEA; Figure 1H) enhanced GLP-1 release, to 1.7- and 3.5-fold of control ($p<0.05$-0.001), respectively. These findings suggest a role for syn1a in L-cell secretion and support use of both the IE-syn1a KO mouse model and AMIC cultures in further studies to assess this hypothesis.

Compared to control animals, IE-syn1a KO mice demonstrated increases in body (Figure 2A) and intestinal (Figure 2B) weight 7-12 days following the completion of daily tamoxifen injections ($p<0.05$-0.001). However, upon normalization of intestinal weight to body weight, the observed increase in intestinal weight was maintained only in male animals lacking syn1a (Figures 2C and S1), suggestive of sexual dimorphism. Morphologic characterization of the

intestinal epithelium further revealed that IE-syn1a KO animals had a small but significant increase in crypt depth ($p<0.01$; Figure 2D). Furthermore, the 39% reduction of syn1a (i.e. *Stx1a*) mRNA observed in intestinal mucosal scrapes from KO animals ($p<0.05$; Figure 2E) was associated with increases in the expression of *Stx1b* and *-2* ($p<0.05$-0.01; Figure 2F). While the function of syn1b in the intestinal epithelium is not known, it appears to play a role in mast cell degranulation (40). In contrast, *Stx2* (*aka* epimorphin) expression in mesenchymal cells abutting the epithelium has been shown to regulate the morphology of the crypt-to-villus axis (41), suggesting a role in the observed increase in crypt depth. Examination of two other syn isoforms that are also localized to the plasma membrane, *Stx3* and *-4* (42), did not reveal any other adaptive changes (Figure 2F).

To determine whether intestinal-epithelial syn1a has any relationship to glucose tolerance, we performed an oral glucose tolerance test (OGTT) in control and IE-syn1a KO mice two-days following completion of tamoxifen or vehicle injection. IE-syn1a KO animals displayed a significant impairment in glucose tolerance, with blood glucose levels reaching 1.3- and 1.4-fold of controls at t=45 ($p<0.05$) and 60 min ($p<0.001$), respectively (Figure 3A). Accordingly, the 2-hr glycemic area-under-the-curve in IE-syn1aKO mice was also significantly increased, to 1.2-fold of controls ($p<0.01$; Figure 3B). Consistent with this finding, IE-syn1a KO mice showed a reduction in plasma insulin levels as compared with controls, which reached statistical significance at t=60 min (Figure 3C). Furthermore, basal GLP-1 levels were 17% lower in IE-syn1a KO mice than in controls ($p<0.05$), with an even further reduction at t=10 min post-oral glucose administration (by 23%, $p<0.05$ vs. basal; $p<0.01$ vs. the difference at t=0 min; Figure 3D). Analyzing these data for sexual dimorphism showed that male but not female IE-syn1a KO animals accounted for the glucose intolerance and reduced plasma insulin levels

observed during the OGTT (Figure S2). However, plasma GLP-1 levels were consistently reduced in both male and female IE-syn1a KO animals (Figure S3A). Gene expression analysis of the GLP-1 prohormone, proglucagon (*Gcg*), in the intestinal mucosa showed no difference between KO and control animals (Figure 2F), indicating that the reduced GLP-1 levels in IE-syn1a KO mice are not due to a deficiency in GLP-1 production. Similar to the reduction in GLP-1 levels, both male and female IE-syn1a KO animals also displayed significantly lower plasma GIP concentrations, by 31 - 53% at t=0, 10 and 60 min ($p<0.05$-0.01; Figures 3E and S3B). Furthermore, a requirement for the incretin hormones in the impaired glucose tolerance of KO animals was confirmed by the demonstration that mice with loss of intestinal-epithelial syn1a had normal glucose tolerance in response to an IPGTT (Figure 3F). Together, these data suggest that the compromised glucose homeostasis in IE-syn1a KO animals occurs, at least in part, as a result of reductions in both GLP-1 and GIP secretion.

To confirm that loss of syn1a impairs L-cell secretory function, AMIC cultures were generated from crypts isolated from IE-syn1a KO and control animals. Interestingly, IE-syn1a KO AMIC cultures were found to have a 78% reduction in *Stx1a* expression ($p<0.01$; Figure 4A). This more profound knock-down in the crypt cultures compared to the mucosal scrapes is likely a consequence of epithelial cell enrichment in the cultures, whereas both villus epithelial and non-villin-expressing syn1a-positive cells contribute to the syn1a signal in the scrapes. We also examined the *Stx1b*, *-2*, *-3* and *-4* isoforms in the AMIC cultures and found no differences in expression (Figure 4B), further suggesting that adaptive changes that were observed in the mucosa were independent of the intestinal-epithelial cells.

Secretion assays with AMIC cultures generated from IE-syn1a KO mice demonstrated no difference in basal GLP-1 secretion as compared to control animals (Figure 4C). However, IE-

syn1a KO mice displayed a 2.6-fold reduction in forskolin-stimulated GLP-1 secretion, to 37% of the response found in controls ($p<0.001$; Figure 4C). Total GLP-1 content of the cultured cells did not differ between the genotypes or treatment groups (Figure 4D). *Gcg* gene expression also did not differ as a result of loss of syn1a (Figure 4B), further suggesting that the reduced GLP-1 secretion is a result of disrupted L-cell secretory function.

To more directly examine the role of syn1a in GLP-1 secretion by the primary L-cell, we initially conducted in vivo and in vitro studies utilizing adenovirus-mediated knockdown of syn1a. However, application of the control adenovirus alone blunted the ability of the intestinal L-cells to respond to known secretagogues, making this an inappropriate model for further study (Figure S4). We therefore crossed the IE-syn1a KO animals with mice expressing Venus under the control of the *Gcg* promoter (35) to permit identification of the L-cell for exocytotic analysis. While Venus-IE-syn1a KO mice did not show any changes in body weight, they were found to have increased intestinal weight which, following normalization to body weight, was maintained only in male animals lacking syn1a (Figures 5A-C and S5). This pattern was very similar to that observed in the IE-syn1a KO mice that did not express *Gcg*-Venus (Figure S1). Furthermore, although *Stx1a* expression was reduced by 58% ($p<0.05$) in the intestinal mucosa (Figure 5D), there were no significant changes in expression of *Stx1b* and *-2* (Figure 5E). However, an OGTT revealed that Venus-IE-syn1a KO animals, like the IE-syn1a KO mice, had impaired glucose tolerance, with significantly elevated glycemia at t=60 min after oral glucose administration in comparison to controls (1.3-fold of control values, $p<0.05$; Figure 5F). Like the IE-syn1a KO mice, these animals also demonstrated sexual dimorphism, with significant changes found only in the male mice (Figure S6). Collectively, these findings suggested an impairment in GLP-1 secretion in the Venus-IE-syn1a KO animals, despite the finding of a 1.8-fold increase in

intestinal mucosal *Gcg* gene expression ($p<0.05$; Figure 5D).

As the heterogonous cell population of both the ileal mucosa and isolated ileal crypt cultures limits our understanding of L-cell specific gene expression, we compiled a syntaxin isoform expression profile from Venus-positive L-cells by RNAseq (Figure 5G). Of the four syn isoforms known to be localized on the plasma membrane, only *Stx1a* appeared to be enriched (by 3.6-fold) in the Venus-positive L-cells as compared to Venus-negative intestinal-epithelial cells. Collectively, these data further suggest a role for syn1a in GLP-1 exocytosis, and validate the use of the Venus-IE-syn1a KO mice as a model for our studies.

As exocytosis by the primary intestinal L-cell has not previously been described, we utilized 2-photon microscopy to visualize SG fusion events in Venus-positive L-cells from both control and Venus-IE-syn1a KO mice, under basal and 50 μM forskolin-stimulated conditions (Figures 6A and S7). In the absence of forskolin, all of the Venus-positive and some of the Venus-negative cells demonstrated periodic exocytotic events; an increase in exocytosis in both cell types was noted upon the addition of forskolin. However, interestingly, some cells demonstrated a profound level of activity as compared to the surrounding cells, with a large granule size that is consistent with the known characteristics of mast cells (Supplemental Video 1) (43). As has been reported for the β-cell (24-29), distinct types of exocytotic events were observed in Venus-positive L-cells from control animals. Thus, throughout the duration of our recordings, we identified both single (full; Supplemental Video 2) and multi-granular (compound; Supplemental Video 3) SG fusions that differed in the size of the signal and the duration of the event (Figure 6A).

The pattern of fusion events observed in L-cells from Venus-control mice was strongly indicative of biphasic exocytosis. Hence, after the basal period, the addition of forskolin

stimulated a 1st-phase of exocytosis at 1-6 min, followed by a 2nd phase at 7-12 min (Figure 6B, D and E). In comparing single L-cells from Venus-IE-syn1a KO and Venus-control mice, there was no obvious change in the number of SG fusion events during the basal period (Figure 6B-E). However, recordings from Venus-IE-syn1a KO L-cells demonstrated that syn1a depletion dramatically reduced the number of SG fusion events under stimulating conditions, such that 1st phase exocytosis was reduced to basal levels ($p<0.05$) and 2nd phase was abolished ($p<0.05$). Finally, determination of the contributions of full and compound fusion events to each phase of secretion revealed that L-cell exocytosis is largely mediated by compound fusion (approximately 75% of total events), under both basal and stimulated conditions (Figure 6D). Importantly, in the absence of syn1a, the reduced number of SG fusion events in both 1st and 2nd phase secretion was attributed to the loss of both full and compound fusion. This result demonstrates the preservation of SG fusion competence under basal conditions but a requirement for syn1a in stimulated SG fusion in the primary L-cell. When taken together, these data illuminate the spatio-temporal activity of the SG exocytosis that underlies GLP-1 secretion.

Discussion

The actions of the incretin hormones, GLP-1 and GIP, account for ~50% of the insulin response to nutrient ingestion (44, 45). However, despite the importance of GLP-1 to glucose homeostasis, major gaps remain in our understanding of the molecular machinery that regulates GLP-1 release. Although studies on the primary L-cell have been limited in the past due, in large part, to the diffuse dispersion of these cells throughout the intestinal epithelium (38), recent advances now permit direct visualization of exocytosis by reporter-labelled L-cells ex vivo following primary culture (35). Using these approaches, the findings of the present study demonstrate the dynamics of SG fusion to the plasma membrane of the primary intestinal L-cell, and the essential role of the core SNARE protein, syn1a, in secretagogue-induced exocytosis of GLP-1.

2-Photon microscopy demonstrated that exocytosis by the primary L-cell is mediated through different types of exocytotic events, of which the majority are compound SG fusion rather than full fusion of single SGs, under both basal and stimulating conditions. These findings contrast to those on the β-cell, for which different types of fusion events occur during different phases of secretion (21-26, 28, 29). Hence, approximately half of 1st phase insulin secretion is mediated by predocked SGs undergoing full fusion (46). In contrast, the sustained, 2nd phase of insulin exocytosis is largely determined by influx of newcomer SGs from the intracellular reserve pool which then undergo mostly full fusion, with only a small contribution attributed to compound exocytosis (24, 28). It is important to note that the use of 2-photon microscopy in the present study precluded determination of any contribution of kiss-and-run exocytosis to GLP-1 secretion, as well as to whether the detected SGs were pre-docked or newcomer, which would be

better observed by total internal reflection fluorescence and electron microscopy. Furthermore, deletion of syn1a from the plasma membrane prevented not only single but also multi-granular fusion events. Indeed, compound fusion may require other isoforms of syn that are expressed in the L-cell (31), as demonstrated for the β-cell (23, 47). However, it is expected that prevention of initial SG fusion with the plasma membrane would preclude detection by 2-photon microscopy of any subsequent SG-to-SG interactions, including not only compound but also sequential fusion events. Thus, the factors that determine the exact nature of exocytotic fusion events in the L-cell remain to be fully defined. However, one signaling pathway that may be involved is Cdc42-dependent reorganization of the actin cytoskeleton that forms a permissive barrier to GLP-1 secretion (48) and which, therefore, may decrease the ability of SGs to move towards the plasma membrane. As a similar mechanism mediates glucose-stimulated exocytosis of newcomer SGs in the β-cell (49, 50), future studies to interrogate the relationships between Cdc42, the actin cytoskeleton and SG dynamics in the intestinal L-cell are warranted. Furthermore, altered β-cell SNARE protein expression in response to gluco- and lipotoxicity is known to affect insulin secretion (51, 52). However, although GLP-1 release is also dysregulated during feeding of a high-fat or Western diet and in association with hyperglycemia caused by circadian disruption (53-55), it currently remains unknown as to whether this is due to changes in expression of syn1a and/or other L-cell SNARE proteins.

Single-cell imaging indicated that GLP-1 secretion by the primary L-cell is biphasic, with the 1st phase occurring 1-6 min after stimulation, and a more sustained 2nd phase at 7-12 min. Interestingly, the isolated rat ileum has previously been noted to demonstrate biphasic release of GLP-1 in response to bethanechol and bombesin, but not calcitonin-gene related peptide, with a 1st peak at 2-4 min and a 2nd phase that is maintained for the duration of the vascular perfusion

(10). Furthermore, re-examination of total internal reflection fluorescence microscopy data from the GLUTag L-cell line also suggests the existence of two phases of exocytosis. Hence, ~0.4 fusions/100 μm^2-30 sec were detected under basal conditions, and this increased to ~1.5 at 1-3 min after KCl-mediated depolarization, followed by a second phase with ~1 event/100 μm^2-30 sec over the ensuing 4-7 min (31). Thus, unlike the β-cell, for which KCl-induced depolarization increases 1st phase secretion, whereas glucose induces biphasic release (21-26, 28, 29), the intestinal L-cell demonstrates biphasic secretion following activation by KCl, forskolin and some, but not all, physiological secretagogues.

As compared to the normal intestine, wherein L-cells constitute ~0.5% of epithelial cells (56), 1.1% of the cells in the AMIC cultures were found to express GLP-1, indicating a relative enrichment in this ileal crypt-cell model. Furthermore, 100% of the AMIC L-cells were found to express syn1a and, of the syntaxin isoforms known to be expressed on the plasma membrane (*Stx1a*, *-1b*, *-2*, *-3, -4*; (42)), only *Stx1a* was found to be enriched. Consistent with an important role for this core SNARE protein in the L-cell, KO of syn1a reduced forskolin-stimulated GLP-1 secretion at both the single-cell and population level in AMIC cultures, and reduced OGTT-induced GLP-1 release in the mouse in vivo. While no profound effects of the KO were found on basal GLP-1 release in the ex vivo and single-cell models examined, basal GLP-1 levels were reduced in vivo as a potential consequence of villin-driven cre expression, resulting in altered release of or responsiveness to paracrine regulators of GLP-1 secretion. Of note, IE-syn1a KO animals demonstrated even greater reductions in basal- and stimulated GIP secretion, likely contributing to the glucose intolerant phenotype through both the reduction of its own insulinotropic actions and via reduced L-cell stimulation by GIP (11). Future studies examining exocytotic dynamics in the GIP-producing K-cell are clearly warranted. Finally, the maintenance

of basal L-cell exocytosis and only partial loss of 1st phase of secretion in the absence of syn1a could suggest contributions by another syn isoform in the L-cell to mediate fusion of pre-docked SGs, with the almost complete loss of 2nd phase secretion explained by the loss of syn1a-mediated newcomer SG fusion, comparable to findings in the β-cell (47). Nonetheless, our previous report of expression of VAMP2 in primary L-cells, a role for VAMP2 in GLP-1 release, and an interaction between VAMP2, syn1a and SNAP25 in the GLUTag cells (31) is consistent with the notion that these proteins form a core SNARE complex in the primary intestinal L-cell.

Although both of the syn1a KO models used in this study were generated from villin-creER$^{T2+/0}$ and syn1a$^{fl/fl}$ mice, small differences were noted in the IE-syn1a KO mice as compared those crossed with the *Gcg*-Venus animals. Hence, the IE-syn1a KO mice demonstrated increases in *Stx1b* and *Stx2* expression. Conversely, the Venus-IE-syn1a KO exhibited an increase only in *Gcg* expression, which could reflect a potential effect of proglucagon-driven Venus expression in the L-cell. However, the subtle differences in gene expression between the KO models was presumed not to influence GLP-1 secretion, as L-cell secretion was found to be impaired by loss of syn1a in both the ex vivo secretion assays (IE-syn1a KO) and single-cell experiments (Venus-IE-syn1a KO). Furthermore, when taken with the rigorous inclusion of multiple genotypes as controls for each of these animal models, our finding of consistent effects of syn1a KO to reduce GLP-1 secretion suggests that these small differences in the mouse models had no impact on the conclusions of this study.

Interestingly, while both male and female animals displayed significantly reduced GLP-1 and GIP levels, IE-syn1a KO mice demonstrated sexual dimorphism in their metabolic responses to oral glucose administration; similar differences in glucose tolerance were also found in the

Venus-IE-syn1a KO animals. The female animals therefore demonstrated an improved capacity to compensate for the reduction in the incretin hormones. However, whether these findings can be extrapolated to humans remains unclear, as a previous study has indicated that OGTT-induced changes in the levels of glucose, insulin and both of the incretin hormones are all increased in women (57).

The mechanisms underlying GLP-1 release from the intestinal L-cell are of increasing interest as a therapeutic approach to the treatment of hyperglycemia in patients with T2D, either alone or in combination with DPP IV inhibition (5-7). Our findings identify an exquisite mechanism of metered secretory output that precisely regulates release of the incretin, GLP-1 and, hence, insulin secretion following a meal. Furthermore, as the intestinal L-cell co-secretes a number of other biologically active peptide hormones, these findings may also have implications in other disease states. The demonstration of a role for syn1a in modulating stimulated SG fusion events provides impetus for further studies to elucidate the full complement of SNARE and cognate accessory proteins in the primary L-cell that mediate distinct exocytotic events, as well as their coupling to the diverse signaling pathways that are activated by nutrient ingestion. Elucidation of the exact mechanisms underlying GLP-1 release holds important implications for development of GLP-1 secretagogues to treat patients with T2D or obesity.

Author Contributions

SEW, HMS, YN, SJH, ABH, FR, FMG and PL researched data. SEW and PLB wrote the manuscript. HMS, YN, SJH, ABH, FR, FMG and HYG reviewed/edited the manuscript.

Acknowledgements

SEW and HMS were supported by Ontario Graduate Scholarships; SEW by Novo-Nordisk Banting and Best Diabetes Centre (BBDC, University of Toronto) Graduate Studentships; YN by a University of Toronto Research Opportunity Summer Studentship; SJH by a BBDC Summer Studentship; and PLB by the Canada Research Chairs program. These studies were supported by an operating grant to PLB from the Natural Sciences and Engineering Research Council of Canada (RGPIN418). The Nikon A1R multi-photon microscope and the Mesoscale Discovery Sector 2400A used in this study was supported by The 3D (Diet, Digestive Tract and Disease) Centre funded by the Canadian Foundation for Innovation and Ontario Research Fund, project number 19442 and 30961. Research in the Reimann/Gribble laboratory was funded by the Wellcome Trust (106262/Z/14/Z, 106263/Z/14/Z) and the Medical Research Council (MRC_MC_UU_12012/3, MRC_MC_UU_12012/5).

Duality of Interest

The authors have no conflicts of interest to report.

Guarantor

PLB takes full responsibility for the content of this manuscript.

References

1. Campbell JE, Drucker DJ. Pharmacology, physiology, and mechanisms of incretin hormone action. *Cell Metab*. 2013;**17**:819-837

2. Dong CX, Brubaker PL. Ghrelin, the proglucagon-derived peptides and peptide YY in nutrient homeostasis. *Nat. Rev. Gastroenterol. Hepatol*. 2012;**9**:705-715

3. Mulvihill EE, Drucker DJ. Pharmacology, physiology, and mechanisms of action of dipeptidyl peptidase-4 inhibitors. *Endocr Rev*. 2014;**35**:992-1019

4. Nauck M. Incretin therapies: highlighting common features and differences in the modes of action of glucagon-like peptide-1 receptor agonists and dipeptidyl peptidase-4 inhibitors. *Diabetes Obes Metab*. 2016;**18**:203-216

5. Brubaker PL. Minireview: Update on incretin biology: focus on glucagon-like peptide-1. *Endocrinology*. 2010;**151**:1984-1989

6. Drucker DJ. Evolving concepts and translational relevance of enteroendocrine cell biology. *J Clin Endocrinol Metab*. 2016;**101**:778-786

7. Pais R, Gribble FM, Reimann F. Stimulation of incretin secreting cells. *Ther Adv Endocrinol Metab*. 2016;**7**:24-42

8. Carr RD, Larsen MO, Jelic K, Lindgren O, Vikman J, Holst JJ, Deacon CF, Ahren B. Secretion and dipeptidyl peptidase-4-mediated metabolism of incretin hormones after a mixed meal or glucose ingestion in obese compared to lean, nondiabetic men. *J. Clin. Endocrinol. Metab*. 2010;**95**:872-878

9. Moller JB, Jusko WJ, Gao W, Hansen T, Pedersen O, Holst JJ, Overgaard RV, Madsen H, Ingwersen SH. Mechanism-based population modelling for assessment of L-cell function based on total GLP-1 response following an oral glucose tolerance test. *J. Pharmacokinet. Pharmacodyn*. 2011;**38**:713-725

10. Dumoulin V, Dakka T, Plaisancie P, Chayvialle J-A, Cuber J-C. Regulation of glucagon-like peptide-1-(7-36)amide, peptide YY, and neurotensin secretion by neurotransmitters and gut hormones in the isolated vascularly perfused rat ileum. *Endocrinology*. 1995;**136**:5182-5188

11. Rocca AS, Brubaker PL. Role of the vagus nerve in mediating proximal nutrient-induced glucagon-like peptide-1 secretion. *Endocrinology*. 1999;**140**:1687-1694

12. Anini Y, Hansotia T, Brubaker PL. Muscarinic receptors control postprandial release of glucagon-like peptide-1: In vivo and in vitro studies in rats. *Endocrinology*. 2002;**143**:2420-2426

13. Parker HE, Adriaenssens A, Rogers G, Richards P, Koepsell H, Reimann F, Gribble FM. Predominant role of active versus facilitative glucose transport for glucagon-like peptide-1 secretion. *Diabetologia*. 2012;**55**:2445-2455

14. Lauffer LM, Iakoubov R, Brubaker PL. GPR119 is essential for oleoylethanolamide-induced glucagon-like peptide-1 secretion from the intestinal enteroendocrine L-cell. *Diabetes*. 2009;**58**:1058-1066

15. Tolhurst G, Heffron H, Lam YS, Parker HE, Habib AM, Diakogiannaki E, Cameron J, Grosse J, Reimann F, Gribble FM. Short-chain fatty acids stimulate glucagon-like peptide-1 secretion via the G-protein-coupled receptor FFAR2. *Diabetes*. 2012;**61**:364-371

16. Habib AM, Richards P, Rogers GJ, Reimann F, Gribble FM. Co-localisation and secretion of glucagon-like peptide 1 and peptide YY from primary cultured human L cells. *Diabetologia*. 2013;**56**:1413-1416

17. Li J, Klughammer J, Farlik M, Penz T, Spittler A, Barbieux C, Berishvili E, Bock C, Kubicek S. Single-cell transcriptomes reveal characteristic features of human pancreatic islet cell types. *EMBO Rep*. 2016;**17**:178-187

18. Rutter GA, Pullen TJ, Hodson DJ, Martinez-Sanchez A. Pancreatic beta-cell identity, glucose sensing and the control of insulin secretion. *Biochem J*. 2015;**466**:203-218

19. Dolai S, Xie L, Zhu D, Liang T, Qin T, Xie H, Kang Y, Chapman ER, Gaisano HY. Synaptotagmin-7 functions to replenish insulin granules for exocytosis in human islet beta-cells. *Diabetes*. 2016;**65**:1962-1976

20. Sudhof TC, Rothman JE. Membrane fusion: grappling with SNARE and SM proteins. *Science*. 2009;**323**:474-477

21. Oh E, Kalwat MA, Kim MJ, Verhage M, Thurmond DC. Munc18-1 regulates first-phase insulin release by promoting granule docking to multiple syntaxin isoforms. *J. Biol. Chem*. 2012;**287**:25821-25833

22. Takahashi N, Hatakeyama H, Okado H, Noguchi J, Ohno M, Kasai H. SNARE conformational changes that prepare vesicles for exocytosis. *Cell Metab*. 2010;**12**:19-29

23. Xie L, Zhu D, Dolai S, Liang T, Qin T, Kang Y, Xie H, Huang YC, Gaisano HY. Syntaxin-4 mediates exocytosis of pre-docked and newcomer insulin granules underlying biphasic glucose-stimulated insulin secretion in human pancreatic beta cells. *Diabetologia*. 2015;**58**:1250-1259

24. Gaisano HY. Here come the newcomer granules, better late than never. *Trends Endocrinol Metab*. 2014;**25**:381-388

25. Takahashi N, Hatakeyama H, Okado H, Miwa A, Kishimoto T, Kojima T, Abe T, Kasai H. Sequential exocytosis of insulin granules is associated with redistribution of SNAP25. *J Cell Biol*. 2004;**165**:255-262

26. Hoppa MB, Jones E, Karanauskaite J, Ramracheya R, Braun M, Collins SC, Zhang Q, Clark A, Eliasson L, Genoud C, Macdonald PE, Monteith AG, Barg S, Galvanovskis J, Rorsman P. Multivesicular exocytosis in rat pancreatic beta cells. *Diabetologia*. 2012;**55**:1001-1012

27. Hanna ST, Pigeau GM, Galvanovskis J, Clark A, Rorsman P, MacDonald PE. Kiss-and-run exocytosis and fusion pores of secretory vesicles in human beta-cells. *Pflugers Arch*. 2009;**457**:1343-1350

28. Gaisano HY. Deploying insulin granule-granule fusion to rescue deficient insulin secretion in diabetes. *Diabetologia*. 2012;**55**:877-880

29. Wang Z, Thurmond DC. Mechanisms of biphasic insulin-granule exocytosis - roles of the cytoskeleton, small GTPases and SNARE proteins. *J. Cell Sci*. 2009;**122**:893-903

30. Gustavsson N, Wang Y, Kang Y, Seah T, Chua S, Radda GK, Han W. Synaptotagmin-7 as a positive regulator of glucose-induced glucagon-like peptide-1 secretion in mice. *Diabetologia*. 2011;**54**:1824-1830

31. Li SK, Zhu D, Gaisano HY, Brubaker PL. Role of vesicle-associated membrane protein 2 in exocytosis of glucagon-like peptide-1 from the murine intestinal L cell. *Diabetologia*. 2014;**57**:809-818

32. Liang T, Qin T, Xie L, Dolai S, Zhu D, Prentice KJ, Wheeler MB, Kang Y, Osborne L, Gaisano HY. New roles of syntaxin-1A in insulin granule exocytosis and replenishment. *J. Biol. Chem.* 2017;**292**:2203-2216

33. el Marjou F, Janssen KP, Chang BH, Li M, Hindie V, Chan L, Louvard D, Chambon P, Metzger D, Robine S. Tissue-specific and inducible Cre-mediated recombination in the gut epithelium. *Genesis*. 2004;**39**:186-193

34. Rowland KJ, Trivedi S, Wan K, Kulkarni RN, Holzenberger M, Robine S, Brubaker PL. Loss of glucagon-like peptide-2-induced proliferation following intestinal epithelial insulin-like growth factor-1 receptor deletion. *Gastroenterology*. 2011;**141**:2166-2175

35. Reimann F, Habib AM, Tolhurst G, Parker HE, Rogers GJ, Gribble FM. Glucose sensing in L cells: a primary cell study. *Cell Metab*. 2008;**8**:532-539

36. Lim GE, Huang GJ, Flora N, LeRoith D, Rhodes CJ, Brubaker PL. Insulin regulates glucagon-like peptide-1 secretion from the enteroendocrine L cell. *Endocrinology*. 2009;**150**:580-591

37. Gagnon J, Baggio LL, Drucker DJ, Brubaker PL. Ghrelin is a novel regulator of GLP-1 secretion. *Diabetes*. 2015;**64**:1513-1521

38. Eissele R, Göke R, Willemer S, Harthus HP, Vermeer H, Arnold R, Göke B. Glucagon-like peptide-1 cells in the gastrointestinal tract and pancreas of rat, pig and man. *Eur. J. Clin. Invest*. 1992;**22**:283-291

39. Schneider CA, Rasband WS, Eliceiri KW. NIH Image to ImageJ: 25 years of image analysis. *Nat Methods*. 2012;**9**:671-675

40. Sander LE, Frank SP, Bolat S, Blank U, Galli T, Bigalke H, Bischoff SC, Lorentz A. Vesicle associated membrane protein (VAMP)-7 and VAMP-8, but not VAMP-2 or VAMP-3, are required for activation-induced degranulation of mature human mast cells. *Eur J Immunol*. 2008;**38**:855-863

41. Fritsch C, Swietlicki EA, Lefebvre O, Kedinger M, Iordanov H, Levin MS, Rubin DC. Epimorphin expression in intestinal myofibroblasts induces epithelial morphogenesis. *J Clin Invest*. 2002;**110**:1629-1641

42. Wheeler MB, Sheu L, Ghai M, Bouquillon A, Grondin G, Weller U, Beaudoin AR, Bennett MK, Trimble WS, Gaisano HY. Characterization of SNARE protein expression in β cell lines and pancreatic islets. *Endocrinology*. 1996;**137**:1340-1348

43. Horiguchi K, Yoshikawa S, Saito A, Haddad S, Ohta T, Miyake K, Yamanishi Y, Karasuyama H. Real-time imaging of mast cell degranulation in vitro and in vivo. *Biochem Biophys Res Commun*. 2016;**479**:517-522

44. Nauck MA, Homberger E, Siegel EG, Allen RC, Eaton RP, Ebert R, Creutzfeldt W. Incretin effects of increasing glucose loads in man calculated from venous insulin and C-peptide responses. *J. Clin. Endocrinol. Metab*. 1986;**63**:492-498

45. Wang Z, Wang RM, Owji AA, Smith DM, Ghatei MA, Bloom SR. Glucagon-like peptide-1 is a physiological incretin in rat. *J. Clin. Invest*. 1995;**95**:417-421

46. Ohara-Imaizumi M, Fujiwara T, Nakamichi Y, Okamura T, Akimoto Y, Kawai J, Matsushima S, Kawakami H, Watanabe T, Akagawa K, Nagamatsu S. Imaging analysis reveals mechanistic differences between first- and second-phase insulin exocytosis. *J. Cell Biol*. 2007;**177**:695-705

47. Zhu D, Koo E, Kwan E, Kang Y, Park S, Xie H, Sugita S, Gaisano HY. Syntaxin-3 regulates newcomer insulin granule exocytosis and compound fusion in pancreatic beta cells. *Diabetologia*. 2013;**56**:359-369

48. Lim GE, Xu M, Sun J, Jin T, Brubaker PL. The Rho guanosine 5'-triphosphatase, Cell Division Cycle 42, is required for insulin-induced actin remodeling and glucagon-like peptide-1 secretion in the intestinal endocrine L cell. *Endocrinology*. 2009;**150**:5249-5261

49. Nevins AK, Thurmond DC. Glucose regulates the cortical actin network through modulation of Cdc42 cycling to stimulate insulin secretion. *Am. J. Physiol Cell Physiol*. 2003;**285**:C698-C710

50. Lam PP, Ohno M, Dolai S, He Y, Qin T, Liang T, Zhu D, Kang Y, Liu Y, Kauppi M, Xie L, Wan WC, Bin NR, Sugita S, Olkkonen VM, Takahashi N, Kasai H, Gaisano HY. Munc18b is a major mediator of insulin exocytosis in rat pancreatic beta-cells. *Diabetes*. 2013;**62**:2416-2428

51. Gaisano HY, Ostenson CG, Sheu L, Wheeler MB, Efendic S. Abnormal expression of pancreatic islet exocytotic soluble N-ethylmaleimide-sensitive factor attachment protein receptors in Goto-Kakizaki rats is partially restored by phlorizin treatment and accentuated by high glucose treatment. *Endocrinology*. 2002;**143**:4218-4226

52. Ostenson CG, Chen J, Sheu L, Gaisano HY. Effects of palmitate on insulin secretion and exocytotic proteins in islets of diabetic Goto-Kakizaki rats. *Pancreas*. 2007;**34**:359-363

53. Gil-Lozano M, Mingomataj EL, Wu WK, Ridout SA, Brubaker PL. Circadian secretion of the intestinal hormone GLP-1 by the rodent L cell. *Diabetes*. 2014;**63**:3674-3685

54. Gil-Lozano M, Wu WK, Martchenko A, Brubaker PL. High fat diet and palmitate alter the time-dependent secretion of glucagon-like peptide-1 by the rodent L-cell. *Endocrinology*. 2016;**157**:586-599

55. Richards P, Pais R, Habib AM, Brighton CA, Yeo GS, Reimann F, Gribble FM. High fat diet impairs the function of glucagon-like peptide-1 producing L-cells. *Peptides*. 2016;**77**:21-27

56. Petersen N, Reimann F, Bartfeld S, Farin HF, Ringnalda FC, Vries RG, van den Brink S, Clevers H, Gribble FM, de Koning EJ. Generation of L cells in mouse and human small intestine organoids. *Diabetes*. 2014;**63**:410-420

57. Vaag AA, Holst JJ, Volund A, Beck-Nielsen H. Gut incretin hormones in identical twins discordant for non-insulin-dependent diabetes mellitus (NIDDM) - Evidence for decreased glucagon-like peptide 1 secretion during oral glucose ingestion in NIDDM twins. *Eur. J. Endocrinol*. 1996;**135**:425-432

Figure Legends

Figure 1: Primary murine intestinal L-cells express syn1a and secrete GLP-1 in vitro. (**A-D**) Mouse intestine (**A**) and AMIC cultures (**B-C**) were immunostained for GLP-1 (red) and syn1a (green); DAPI is blue, negative controls are shown in the inset, and arrows indicate GLP-1-positive cells. Representative images are shown from n=6 IE-syn1a control (**A-B**) mice, and from n=4 IE-syn1a KO animals (**C**). Quantification of control and IE-syn1a KO AMIC L-cell syntaxin-1a immunofluorescence intensity (**D**; n=4 cells from 4 control mice and n=6 cells from 5 IE-syn1a KO mice). (**E-H**) AMIC cultures from C57Bl/6 mice were treated for 2hr with forskolin/IBMX (**E-F**; n=10-11), or varying concentrations of GIP (**G**; n=7-12) or OEA (**H**; n=5-7) with forskolin as the positive control. GLP-1 secretion as a percent of total content and total GLP-1 content for the same cultures are shown in (**E-F**), respectively. * $p<0.05$, ** $p<0.01$ and *** $p<0.001$ vs. vehicle control.

Figure 2: IE-syn1a KO mice demonstrate small intestinal adaptive responses. (**A-C**) Body weight (**A**), small intestinal weight (**B**), and small intestinal weight normalized to body weight (**C**) in male and female control and IE-syn1a KO mice (n= 10-13). (**D**) Crypt depth and villus height in control and IE-syn1a KO mice (n=5-8). (**E-F**) *Stx1a* (**E**) and *Stx* isoform and *Gcg* (**F)** transcript levels in ileal mucosal scrapes from control and IE-syn1a-KO mice (n=10-13). * $p<0.05$, ** $p<0.01$ and *** $p<0.001$ vs. control mice.

Figure 3: IE-syn1a KO mice demonstrate reduced GLP-1 secretory responses during an OGTT in association with impaired glucose tolerance. (**A-E**) Male and female control and IE-syn1a KO mice (n=8-22) were administered an OGTT at t=0 min followed by blood sampling at 0, 10, 60,

90 and 120 min; a second cohort of mice (n=7-10) also included sampling for blood glucose at t = 30 and 45 min. Blood glucose (**A**), glycemic area-under-the-curve (AUC, **B**) and levels of plasma insulin (**C**), GLP-1 (**D**; plasma GLP-1 levels were normalized to control levels at t=0 min (20.8 ± 3.1 pg/ml; n=25) to account for variance found between two different assay plates) and GIP (**E**). (**F**) Separate cohorts of male and female mice (n=6) were administered an IPGTT at t=0 min followed by blood sampling for determination of blood glucose. * $p<0.05$, ** $p<0.01$ and *** $p<0.001$ vs. control mice or as indicated for the delta response.

Figure 4: AMIC cultures from IE-syn1a KO mice demonstrate reduced GLP-1 secretory responses. (**A-B**) *Stx1a* (**A**) and *Stx* isoform and *Gcg* (**B**) transcript levels in AMIC cultures from male and female control and IE-syn1a KO mice (n=4-6). (**C-D**) Control and IE-syn1a KO AMIC cultures were treated for 2 hr with vehicle (basal) or forskolin plus IBMX (n=7-9), followed by determination of GLP-1 release into the media (**C**; control basal secretion was 5.9 ± 2.2% of total cell content) and (**D**) GLP-1 content in the media plus cells. ** $p<0.01$ and *** $p<0.001$ vs. basal; ### $p<0.001$ vs. same treatment in controls.

Figure 5: Venus-IE-syn1a KO mice demonstrate impaired glucose tolerance during an OGTT. (**A-C**) Body weight (**A**), small intestinal weight (**B**) and small intestinal weight normalized to body weight (**C**) in male and female control and IE-syn1a-KO mice. (**D-E**) mRNA transcript levels for *Stx1a* (**D**) and *Stx* isoforms and *Gcg* (**E**) in ileal mucosal scrapes from control and IE-syn1a-KO mice. (**F**) Control and IE-syn1a KO mice were administered an OGTT at t=0 min followed by blood sampling for determination of blood glucose levels (n=9-12 for **A-F**). (**G)** RNAseq for syntaxin isoforms in FACS-isolated $Venus^+$ vs. $Venus^-$ jejunal/ileal epithelial cells

from female *Gcg*-Venus mice (inset shows expanded scale; n=3). FPKM, fragments per kilobase of exon per million fragments mapped.

Figure 6: 2-Photon microscopy of primary ileal L-cells demonstrates the role of syn1a in multiple forms of exocytosis. (**A**) Representative images and fluorescent intensity tracings of single/full SG and multi-granular/compound SG fusion events in Venus-positive L-cells from control mice. (**B-E**) Quantification of the total number of fusion events collected over a 3 min basal period and a 12 min forskolin infusion period in control (**B**) and Venus-IE-syn1a KO (**C**) mice; (**D**) indicates the same data binned into different phases of secretion (basal: t = -3 to -1 min; 1st phase: t = 1 to 6 min; and 2nd phase: t = 7 to 12 min) and then classified as full vs. compound fusion. The dotted line in (**B**) indicates best-fit curve for stimulated exocytosis (R^2 = 0.82). *p<0.05, ** p<0.01 and *** p<0.001 vs. basal; # p<0.05 and ### p<0.001 vs. the same phase in control mice, for total fusion events. (**E**) Cumulative total fusion events. * p<0.05, ** p<0.01 for each time point at t = 4-12 min. n= 9 cells from 6 control mice and 6 cells from 3 IE-Venus-syn1a KO.

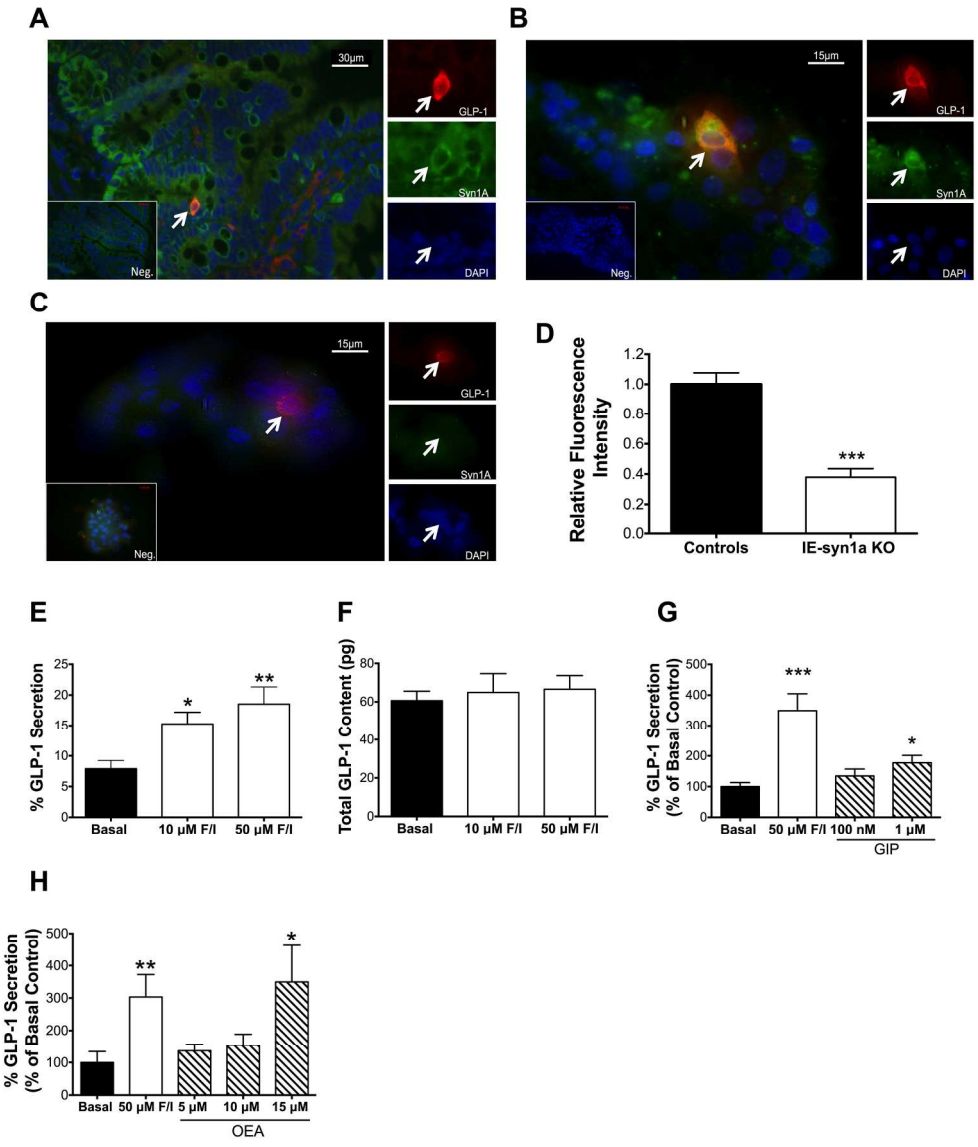

Figure 1

208x240mm (300 x 300 DPI)

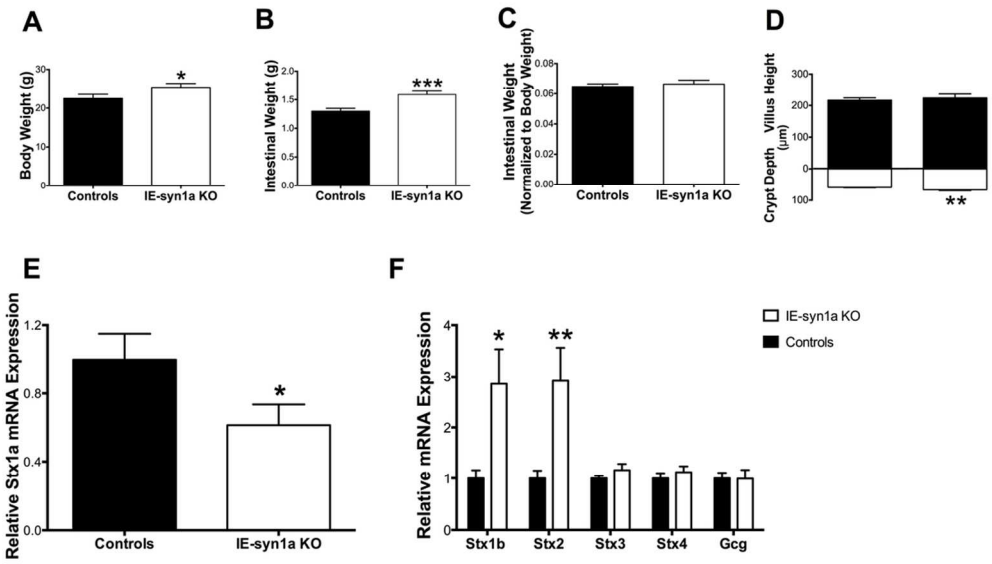

Figure 2

103x59mm (300 x 300 DPI)

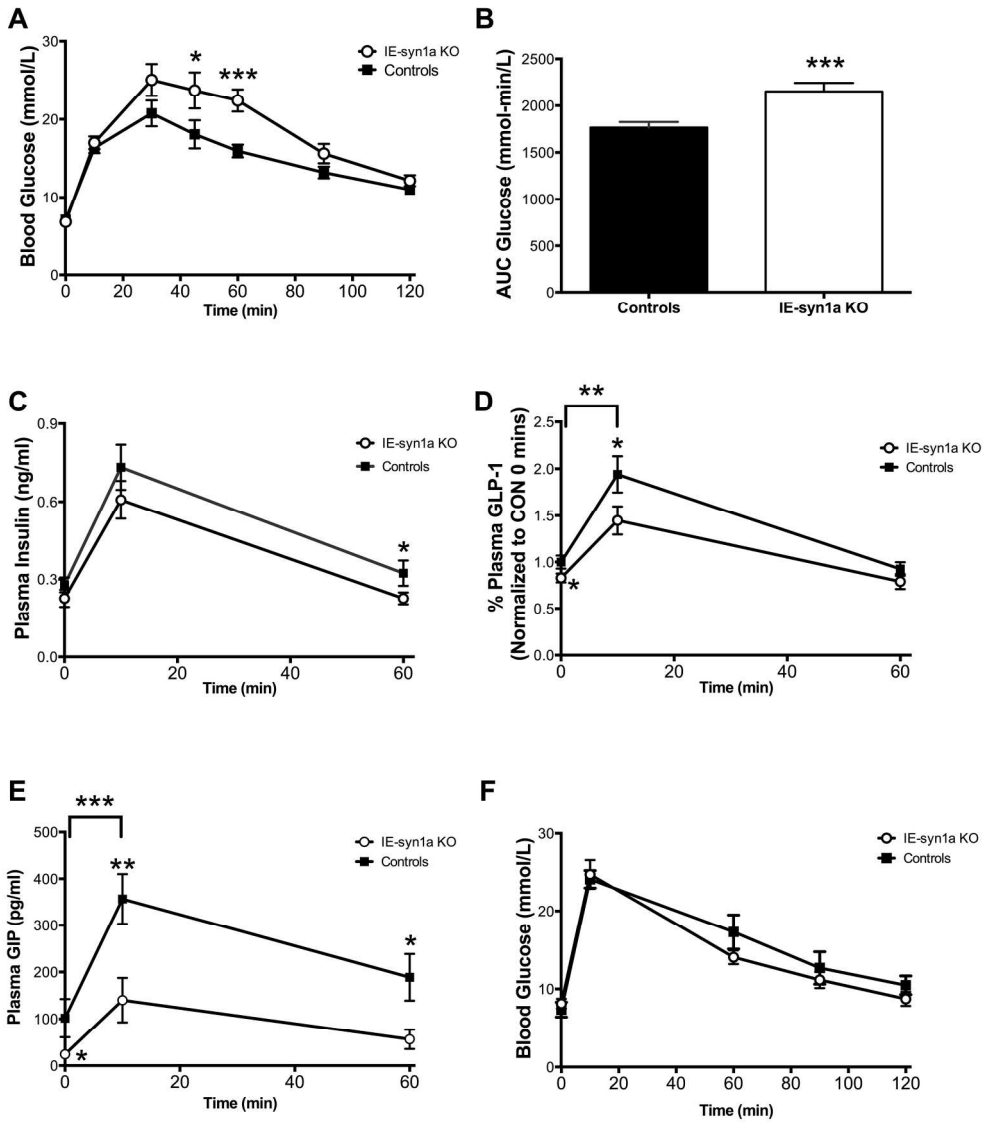

Figure 3

201x229mm (300 x 300 DPI)

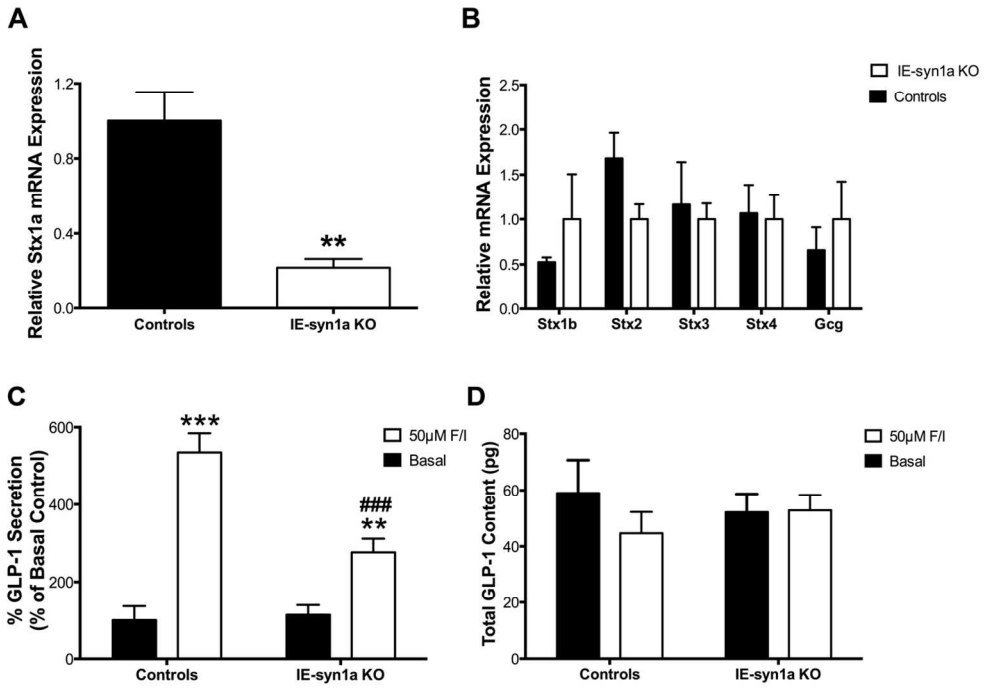

Figure 4

125x88mm (300 x 300 DPI)

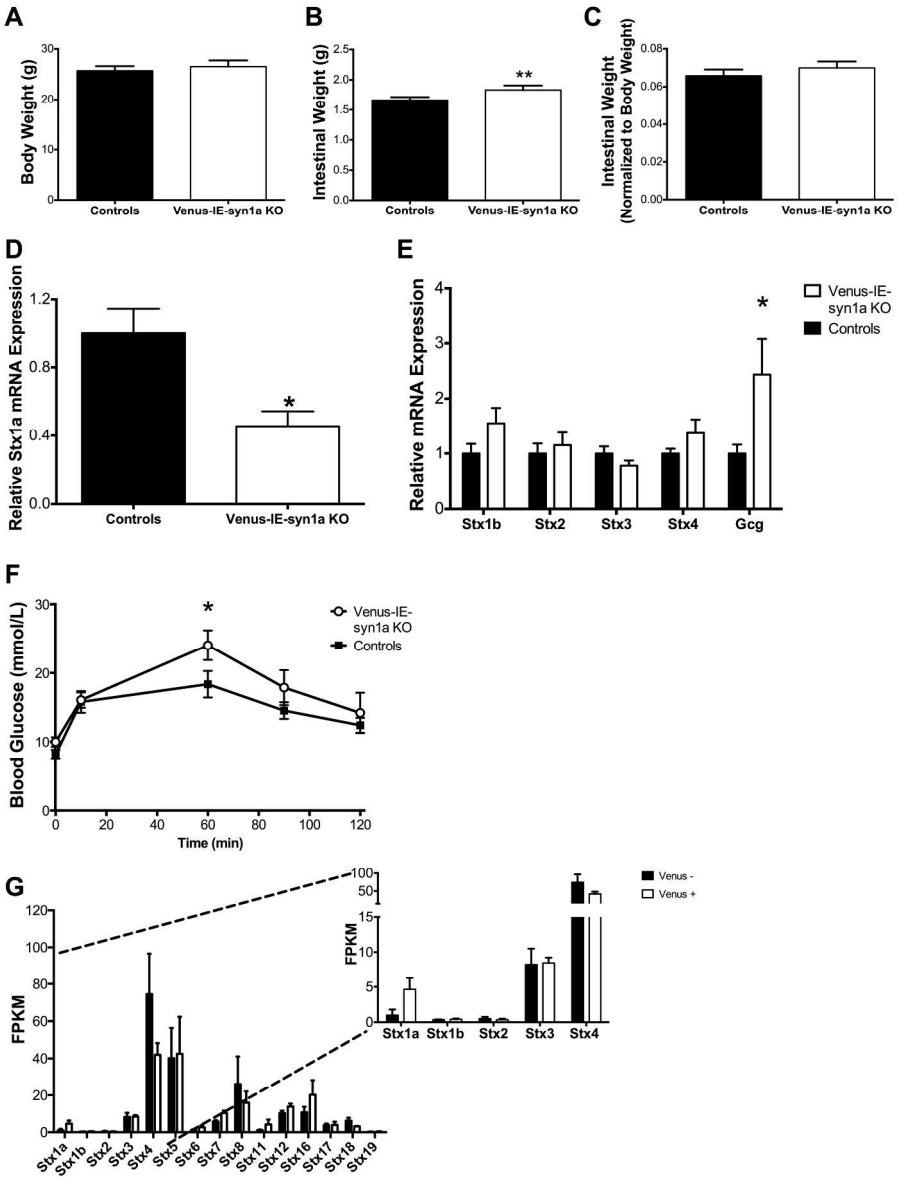

Figure 5

229x294mm (300 x 300 DPI)

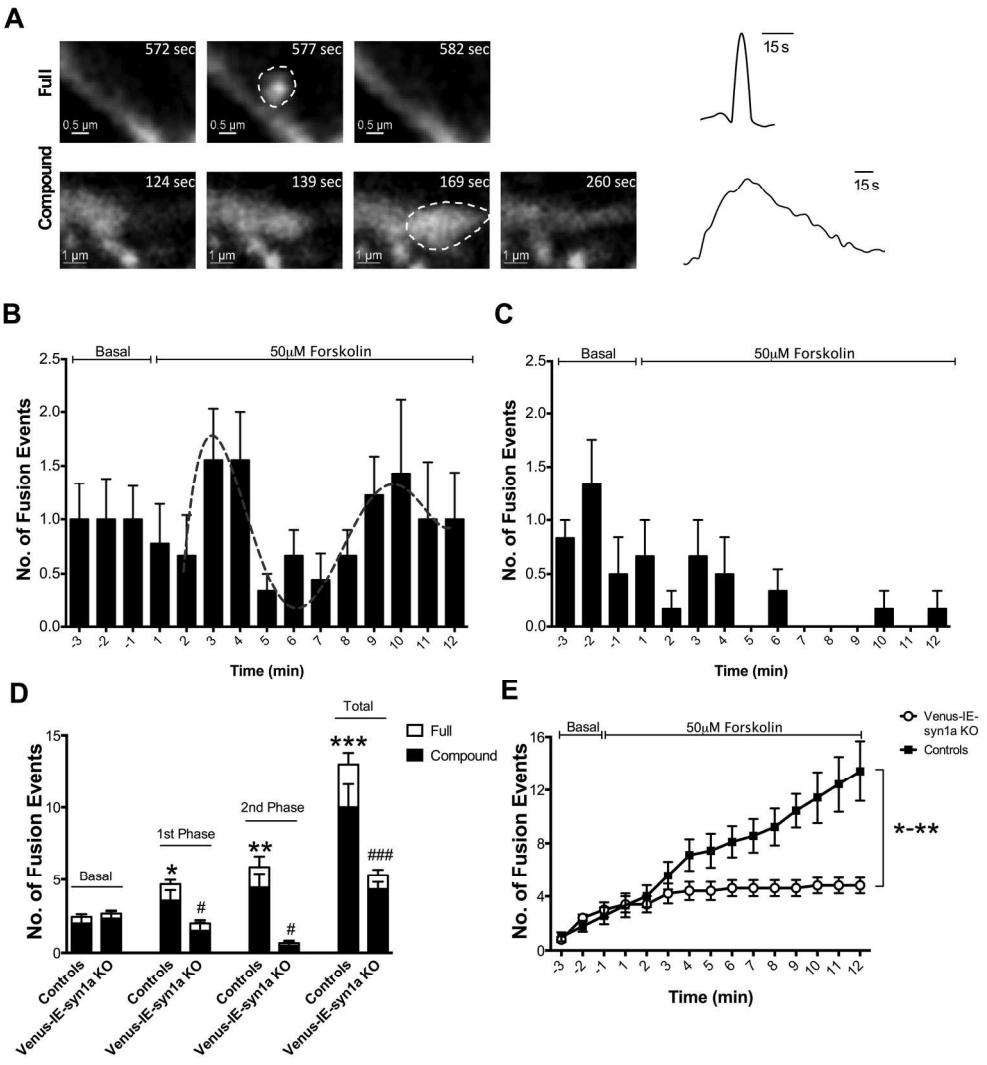

figure 6

192x208mm (300 x 300 DPI)

SUPPLEMENTAL TABLES

Table S1: Genotyping primers

Gene	Forward	Reverse	Amplicon (bp)	Annealing Temperature (^{O}C)
Stx1a	GCT GCA GAA GCA AGA GAA CC	CAG CCA TAC AAA AAC CAC CA	WT: 404 Flox: 239	50.0
Cre	CAA GCC TGG CTC GAC GGC C	CGC GAA CAT CTT CAG GTT CT	390	50.0
Gcg/GFP	AAT TGA GCT CAT TTG GAC TGC C	CTT GCC GTA GGT GGC ATC G	210	50.0
GFP/GFP	CTG GTA GTG GTC GGC GAG C	GTT CAG CGT GTC CGG CGA G	470	50.0

Table S2: Antibody table

Sample	Antigen	Primary Antiserum	Secondary Antiserum
Ileal Tissue	Syntaxin1a	Rabbit anti-syn1a, 1:500 (Abcam cat#41453)	AlexaFluor488-goat anti-rabbit IgG, 1:150 (Life Technologies)
	GLP-1	Mouse anti-GLP-1, 1:400 (Abcam cat # 23472)	AlexaFluro555-goat anti-mouse IgG, 1:150 (Life Technologies)
AMIC Culture	Syntaxin1a	Rabbit anti-syn1a, 1:1000 (Abcam cat#41453)	AlexaFluor488-goat anti-rabbit IgG, 1:150 (Life Technologies)
	GLP-1	Mouse anti-GLP-1, 1:200 (Abcam cat # 23472)	AlexaFluro555-goat anti-mouse IgG, 1:150 (Life Technologies)

Table S3: qRT-PCR Primer/Probes (all from Applied Biosystems)

Transcript	Product number	Exons targeted
Gcg	Mm00801714_m1	5-6
H3f3a	Mm01612808_g1	3-4
Stx1a	Mm00444008_m1	1-2
Stx1b	Mm01275274_m1	1-2
Stx2	Mm04229900_m1	2-3
Stx3	Mm01197689_m1	6-7
Stx4	Mm00436827_m1	5-6

SUPPLEMENTAL FIGURE AND VIDEO LEGENDS

Figure S1: Body weight (**A**), intestinal weight (**B**) and intestinal weight normalized to body weight (**C**) in the male vs. female control and IE-syn1a KO mice shown in Figure 2.

Figure S2: Blood glucose (**A**), and plasma insulin (**B**) levels in the male vs. female control and IE-syn1a KO mice shown in Figure 3.

Figure S3: Plasma GLP-1 (**A**), and GIP (**B**) levels in the male vs. female control and IE-syn1a KO mice shown in Figure 3.

Figure S4: (**A-B**) Male C57Bl/6 mice were administered ileal AdV-RFP (control) or AdV-iCre followed by intra-ileal administration of OEA 2 d later, and determination of mucosal *Stx1a* mRNA transcript levels (**A**) and plasma GLP-1 levels (**B**; n=3-4). (**C-D**) AMIC cultures from male C57Bl/6 mice were treated with AdV-RFP (control) or AdV-iCre for 2 d, followed by 2 hr treatment with vehicle (basal), forskolin plus IBMX or OEA for 2 hr, and determination of cell *Stx1a* mRNA transcript levels (**C**) and GLP-1 content in the media and cells (**D**; n=4).

Figure S5: Body weight (**A**), intestinal weight (**B**) and intestinal weight normalized to body weight (**C**) in the male vs. female control and Venus-IE-syn1a-KO mice shown in Figure 5.

Figure S6: Blood glucose levels in the male vs. female control and Venus-IE-syn1a KO mice shown in Figure 5.

Figure S7: Representative 2-photon images of full and compound fusion events using SRB (red) and Venus (green), as visualized in the respective cells shown in Figure 6A.

Supplemental Video 1: Full-field view of a $Venus^+$ L-cell (green) surrounded by unlabelled cells. Forskolin was added at t = 30 sec. Note the large granule size and multiple fusion events occurring in a single neighbouring cell (arrow), consistent with the known properties of mast cells. The same video is submitted in both .avi and .mp4 format.

Supplemental Video 2: Single granule, full fusion event at t = 577.8 sec in the membrane of a $Venus^+$ L-cell. The same video is submitted in both .avi and .mp4 format.

Supplemental Video 3: Multi-granular, compound fusion event at t = 129.3 – 255.3 sec in the membrane of a $Venus^+$ L-cell. The same video is submitted in both .avi and .mp4 format.

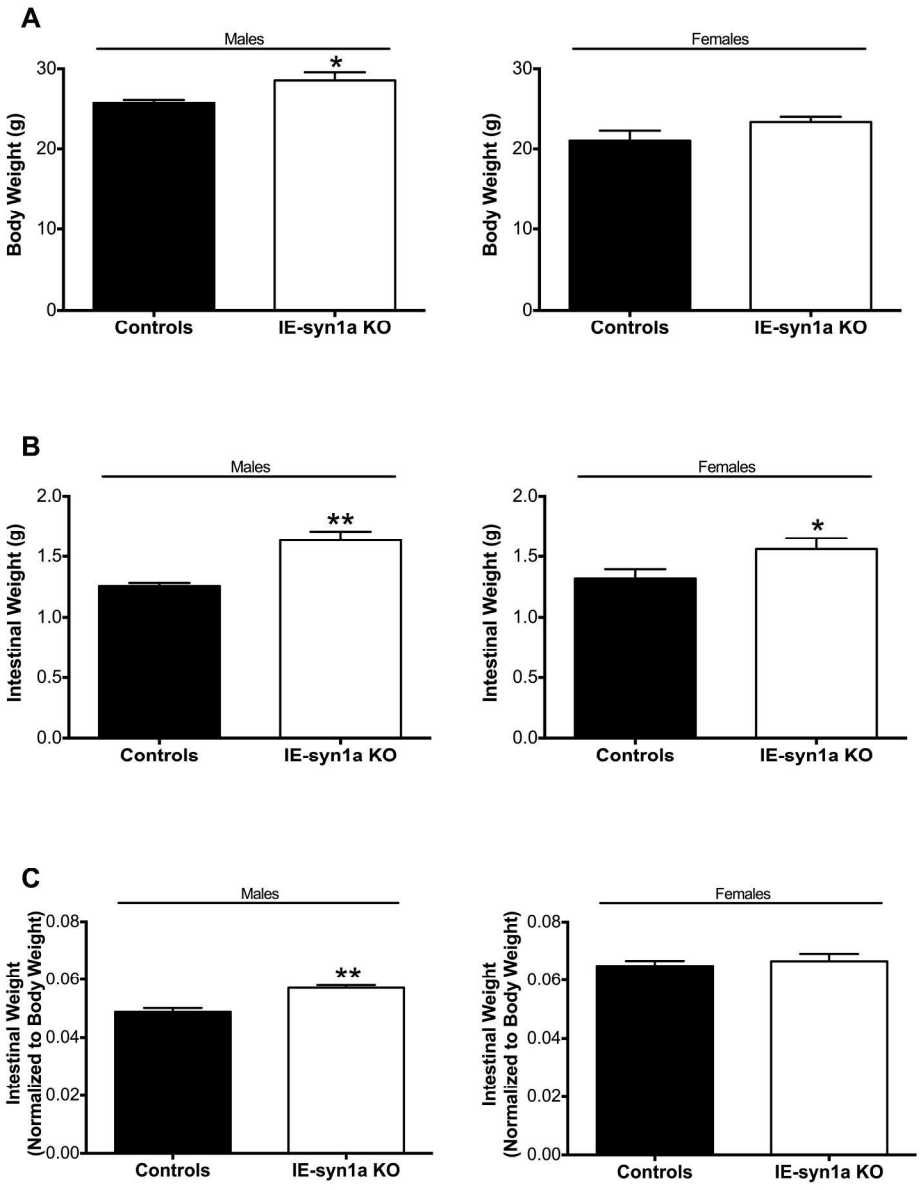

218x267mm (300 x 300 DPI)

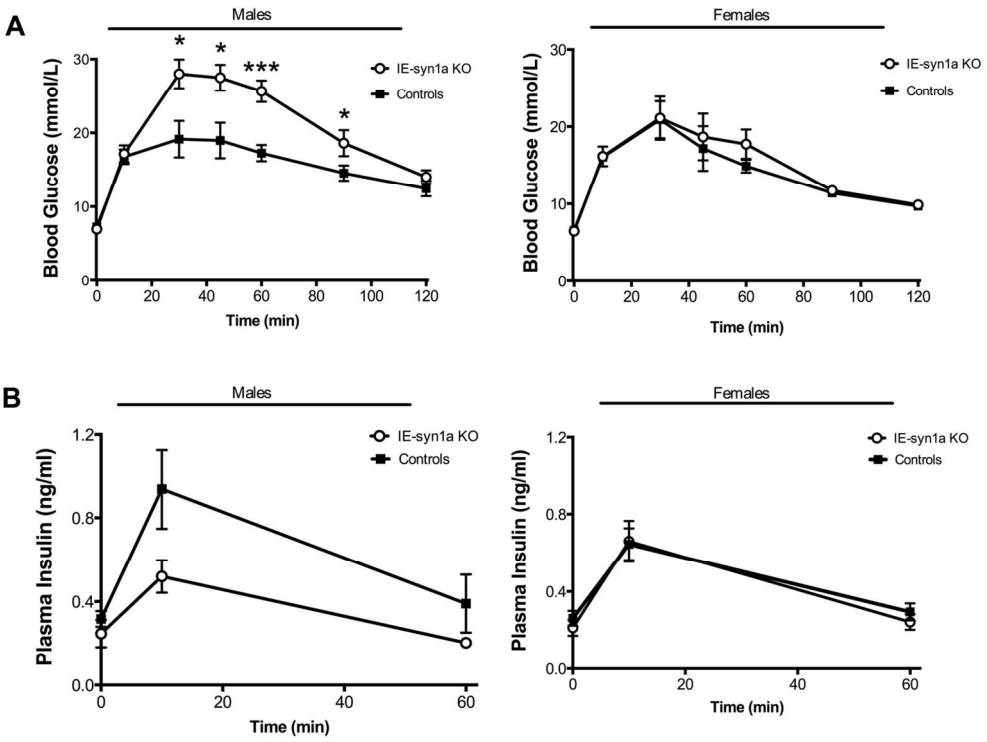

134x101mm (300 x 300 DPI)

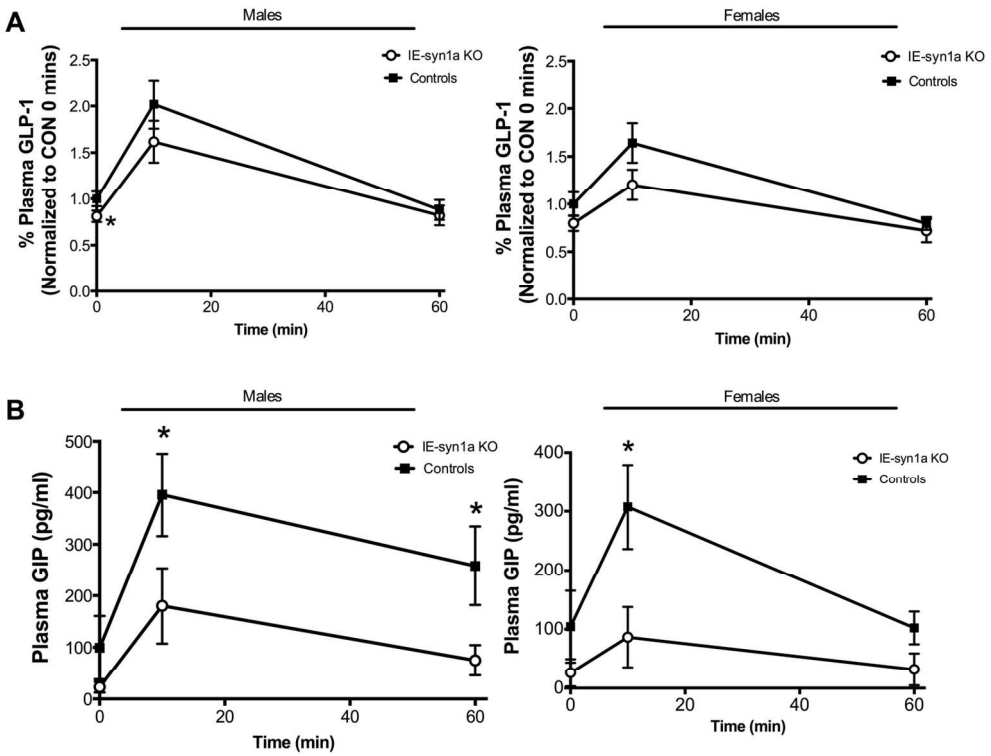

139x106mm (300 x 300 DPI)

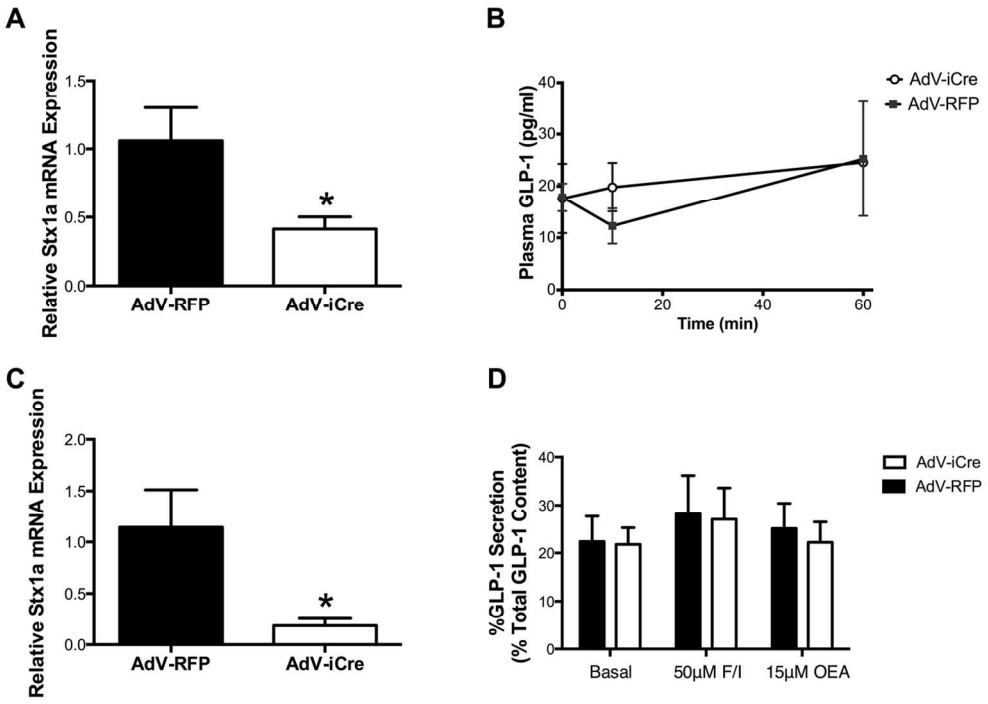

130x94mm (300 x 300 DPI)

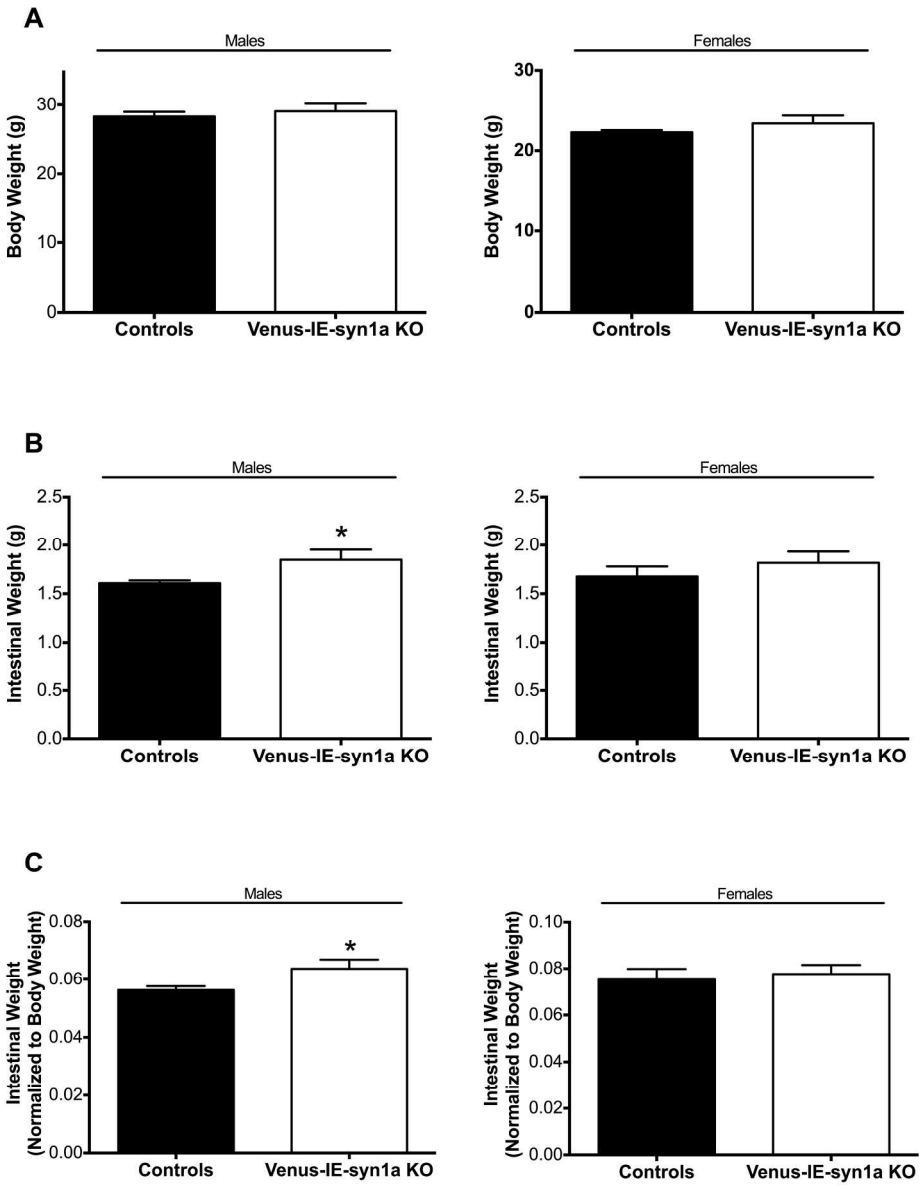

218x266mm (300 x 300 DPI)

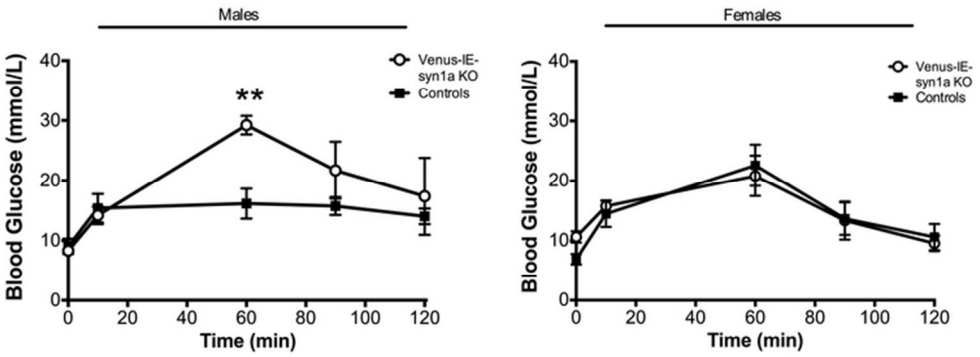

65x24mm (300 x 300 DPI)

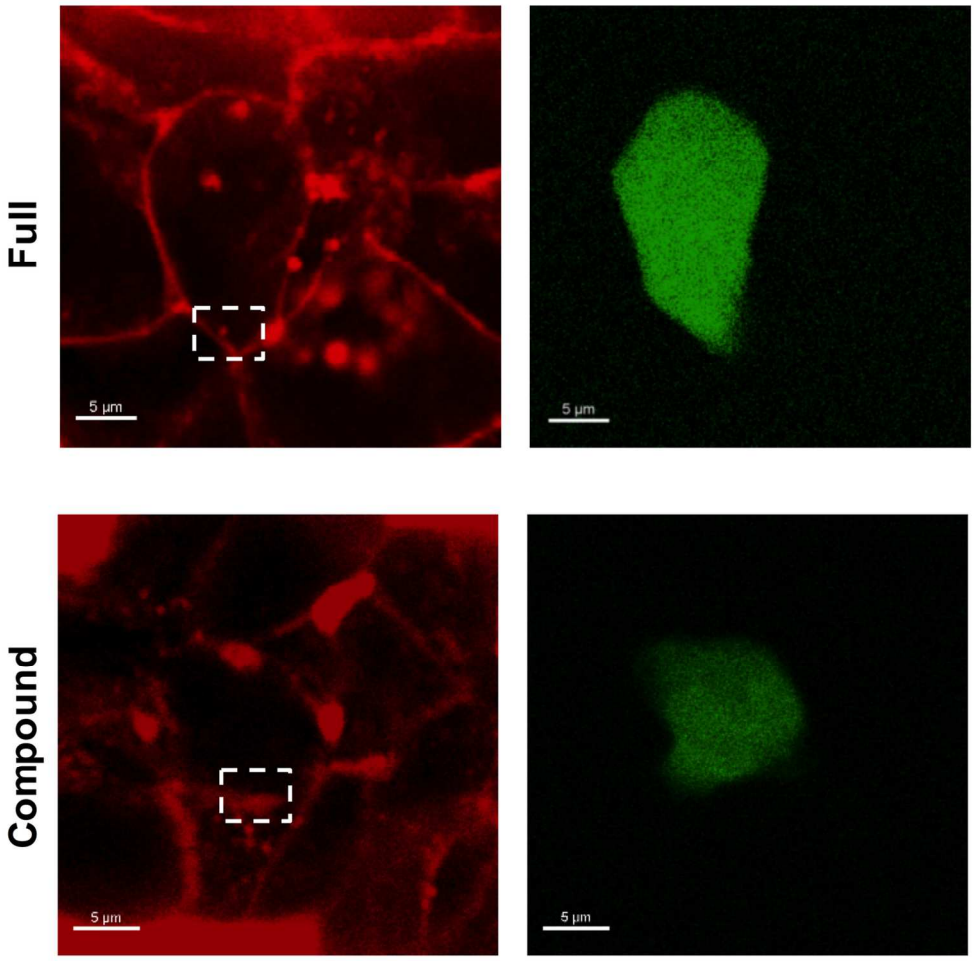

129x130mm (300 x 300 DPI)

The SNARE protein, syntaxin1a, plays an essential role in biphasic exocytosis of the incretin hormone, glucagon-like peptide-1

Sarah E. Wheeler[1], Holly M. Stacey[1], Yasaman Nahaei[1], Stephen J. Hale[1], Alexandre B. Hardy[2], Frank Reimann[3], Fiona M. Gribble[3], Pierre Larraufie[3], Herbert Y. Gaisano[1,4] and Patricia L. Brubaker[1,4]

Departments of [1]Physiology and [4]Medicine, University of Toronto, Toronto, ON M5S 1A8, Canada; [2]3D CFI Centre, University of Toronto, Toronto, ON M5S 1A8, Canada; and [3]Wellcome Trust-MRC Institute of Metabolic Science, Metabolic Research Laboratories, University of Cambridge, Addenbrooke's Hospital, Box 289, Hills Rd, Cambridge, CB2 0QQ, United Kingdom.

Running title: Role of syntaxin-1a in biphasic GLP-1 secretion

Corresponding Author: Dr. P.L. Brubaker, Rm 3366 Medical Sciences Building, University of Toronto, 1 King's College Circle, Toronto, ON M5S 1A8, Canada. Tel: 1-416-978-2593; email p.brubaker@utoronto.ca

Metrics: Abstract, 200 words; Text, 4,497 words; References, 57; Figures 6; Supplementary Figures, 7; Supplementary videos, 6; Supplementary tables, 3.

Abstract

Exocytosis of the hormone, glucagon-like peptide-1 (GLP-1), by the intestinal L-cell is essential for the incretin effect after nutrient ingestion, and is critical for the actions of dipeptidylpeptidase IV inhibitors that enhance GLP-1 levels in patients with type 2 diabetes. 2-Photon microscopy revealed that exocytosis of GLP-1 is biphasic, with a 1st peak at 1-6min and a 2nd peak at 7-12min after stimulation with forskolin. Approximately 75% of the exocytotic events were represented by compound granule fusion, and the remainder were accounted for by full fusion of single granules, under basal and stimulated conditions. The core SNARE protein, syntaxin-1a (syn1a), was expressed by murine ileal L-cells. At the single L-cell level, 1st phase forskolin-induced exocytosis was reduced to basal ($p<0.05$) and 2nd phase exocytosis was abolished ($p<0.05$) by syn1a knockout. L-cells from intestinal-epithelial syn1a-deficient mice demonstrated a 63% reduction in forskolin-induced GLP-1 release in vitro ($p<0.001$), and a 23% reduction in oral glucose-stimulated GLP-1 secretion ($p<0.05$) in association with impairments in glucose-stimulated insulin release (by 60%, $p<0.01$) and glucose tolerance (by 20%, $p<0.01$). Our findings therefore identify an exquisite mechanism of metered secretory output that precisely regulates release of the incretin hormone, GLP-1 and, hence, insulin secretion following a meal.

Keywords: 2-photon microscopy, exocytosis, GIP, GLP-1, GLP-2, intestine, knockout, OGTT, oxyntomodulin, primary cells, proglucagon-Venus, secretion, villin-cre

Introduction

The incretin hormone, glucagon-like peptide-1 (GLP-1), plays an essential role in the maintenance of normoglycemia, through enhancement of glucose-dependent insulin secretion and suppression of glucagon release, gastric emptying and appetite (1, 2). As a consequence of these beneficial actions, GLP-1 receptor agonists are now widely-utilized to treat patients with type 2 diabetes (T2D) and obesity. In contrast to the actions of GLP-1-derivative drugs, therapeutic dipeptidylpeptidase IV (DPP IV) inhibitors prevent the degradation of endogenously-secreted GLP-1, as well as of the other incretin hormone, glucose-dependent insulinotropic peptide (GIP) (3, 4). The possibility of utilizing GLP-1 secretagogues, alone or in combination with DPP IV inhibition, has therefore engendered considerable interest as a new approach to incretin therapy (5-7).

~~GLP-1~~Hormone secretion by the intestinal L-cell which includes, not only GLP-1 but also the related peptides, GLP-2 and oxyntomodulin, demonstrates two peaks of release following nutrient ingestion (8, 9). Rodent studies have demonstrated that part of the early peak of GLP-1 secretion is mediated indirectly, through vagal pathways originating in the duodenum that activate muscarinic receptors on the distal L-cell (10-12). In contrast, the later peak of GLP-1 release is initiated by direct contact of luminal nutrients with the L-cell, resulting in transporter- and ion channel-mediated depolarization, as well as activation of multiple G protein-coupled receptors (13-16). Many of these receptors are expressed not only by the intestinal L-cell, but also by the pancreatic β-cell (17), consistent with the coordinated release of GLP-1 and insulin in vivo. However, in contrast to the β-cell, for which the signaling pathways regulating insulin secretion are well-established (18), much less is known about the intestinal L-cell.

Glucose-mediated depolarization of the β-cell opens voltage-gated calcium channels, thereby activating the calcium-sensor, synaptotagmin-7 (19). This relieves the clamping action of synaptogamin-7 on the SNARE fusion machinery, which consists of the vesicle SNARE protein, VAMP, and the plasma membrane SNAREs, syntaxin (syn) and SNAP23/25 (20), thus permitting insulin exocytosis. Although the β-cell expresses several SNARE isoforms, VAMP2 and syn1a are most important for 1st phase glucose-stimulated insulin secretion (GSIS), with VAMP8 and syn3/4 contributing to both 1st and 2nd phase release (21-23). The SNARE proteins also mediate several different types of exocytotic events in the β-cell. Thus, predocked secretory granules (SGs) contribute predominantly to 1st phase secretion, whereas newcomer granules recruited from an intracellular reserve pool account for some of 1st phase and practically all of 2nd phase insulin exocytosis (24). Furthermore, these SGs also undergo temporally and physically distinct types of fusion with the plasma membrane, termed full, sequential, compound and kiss-and-run (24-29).

While one study has demonstrated a role for synaptotagmin-7 in GLP-1 secretion (30), little is known about the role of the core SNARE proteins in the L-cell. We have reported that the murine GLUTag L-cell line expresses multiple isoforms of VAMP and syn, as well as SNAP25 (31). VAMP2 was demonstrated to play an ~~essential~~ important role in GLP-1 secretion by these cells, and was also found to be expressed in primary mouse intestinal L-cells. Furthermore, VAMP2 co-immunoprecipitates with syn1a and SNAP25 in the GLUTag cells, suggesting these SNARE proteins form a functional exocytotic complex in the L-cell. Given the current interest in therapeutic approaches to enhance release of GLP-1 into the circulation (5-7), we have now utilized novel knockout mouse models in vivo and ex vivo, in combination with single-cell visualization of exocytosis, to interrogate GLP-1 release by the primary intestinal L-cell. We

show that GLP-1 release is biphasic, as mediated primarily by multi-granular (i.e. compound) fusion under both basal and stimulated conditions, and that the SNARE protein, syn1a, plays an essential role in the exocytosis of GLP-1. These findings identify novel regulatory mechanisms that underlie secretion of the incretin hormone, GLP-1, and have implications to the development of GLP-1 secretagogues for therapeutic use in the treatment of T2D and obesity.

Methods

Animals Male C57Bl/6 mice (7-12 wk) were from Charles River. Female syn1a$^{fl/fl}$ (32) were crossed with male villin-creER$^{T2+/0}$ (B6-Tg(Vil-cre/ERT2)23Syr) (33, 34) mice and the resultant tamoxifen-inducible intestinal-epithelial syn1a$^{fl/fl}$;villin-creER$^{T2+/0}$ (IE-syn1a KO) animals were crossed with proglucagon (*Gcg*)-Venus mice (35) to generate Venus-IE-syn1a KO animals (see Table S1 for primers). Age- (7-12 wk) and sex-matched male and female littermates were studied, and controls included: vehicle- and tamoxifen (1 mg/100 µl sunflower oil, ip for 5 d)-treated syn1a$^{fl/fl}$, villin-creER$^{T2+/0}$, syn1a$^{fl/-}$;villin-creER$^{T2+/0}$ and syn1a$^{fl/-}$;villin-creER$^{T2+/0}$;*Gcg*-Venus mice, as well as vehicle-treated syn1a$^{fl/fl}$;villin-creER$^{T2+/0}$ and syn1a$^{fl/fl}$;villin-creER$^{T2+/0}$;*Gcg*-Venus animals, as appropriate for the KO model being studied. Two-three days after induction, mice were fasted overnight followed by an oral or intraperitoneal glucose tolerance test (OGTT: 5g/kg glucose; as previously shown to optimize GLP-1 release in mice (36); and IPGTT: 3 g/kg glucose, as determined in pilot studies to match the glycemic response observed in the OGTT, data not shown) and tail-vein blood collection. Glycemia was determined using a glucose meter (OneTouch, LifeScan), and plasma total GLP-1 (Mesoscale Discovery), total GIP (Millipore) and insulin (Crystal Chem) by kit-assay, as reported (37). Due to their high concentration of L-cells (38), ileal segments were collected for primary culture and analyses. All animal protocols were approved by the Animal Care Committee of the University of Toronto.

Adult mouse ileal crypt (AMIC) cultures Isolated crypts from 10-cm mouse ileum were plated overnight, as reported (35). Two-hr secretion assays were followed by ELISA (Millipore) for active GLP-1 levels in media and cells, as reported (12, 35). Secretion was calculated as the

percent of total culture content that was detected in the media. Experiments were conducted in quadruplicate wells to make n=1 per mouse.

2-Photon microscopy was performed on AMIC cultures perfused at 2 ml/min and 30 ^{o}C. Sulforhodamine-B (0.8 mM) (25) was added 2-3 min prior to visualization using a Nikon A1R multi-photon microscope, for up to 3 min (basal) followed by 12 min with 50 μM forskolin. L-cells were identified by Venus (YFP) fluorescence, and the cell membrane was defined by the extracellular localization of sulforhodamine-B. Data were analysed with NIS-Elements software (Nikon). Focal events that occurred over ≤10 sec were classified as full fusion, whereas events of longer duration were considered to be compound fusion.

Morphometric and immunometric analyses Crypt-villus height was measured in hematoxylin & eosin-stained ileal sections in a minimum of 20 well-oriented axes per mouse. Ileal sections and AMIC cultures were stained for syn1a and GLP-1 (see Table S2 for antibodies), followed by visualization using a Zeiss deconvolution microscope and analysis of fluorescence intensity using ImageJ# (39). Negative controls omitted the primary antisera.

Molecular analyses Ileal Venus^{+} and Venus^{-} cells were collected from female *Gcg*-Venus mice (n=3) by fluorescence-activated cell sorting. Barcode-ligation and end repair were achieved using the Ovation Rapid DR Multiplex System 1–96 (NuGEN). Combined barcoded libraries underwent SE50 sequencing using an Illumina HiSeq 2500 system (Genomics Core Facility, Cancer Research UK Cambridge Institute). Sequence reads were demultiplexed using the Casava pipeline (Illumina) and aligned to the mouse genome (GRCm38) using Tophat-v2.1.0 (http://ccb.jhu.edu/software/tophat/index.shtml). Differential gene expression was determined using Cufflinks-v2.2.1 (http://cole-trapnell-lab.github.io/cufflinks/), as reported (35).

Total RNA from ileal mucosal scrapes and AMIC cultures was reverse-transcribed and analyzed by PCR with primer/probe sets from Applied Biosystems (Table S3). Histone 3A was used as the internal control for analysis by the ΔΔCt method.

Adenovirus studies: Syn1a$^{fl/fl}$ mice were anesthetized, laparotomized and 0.75 ml of 0.9-1.8x10^{8} infection units/ml Adenovirus-RFP-improved cre-recombinase (Adv-iCre) or Adv-RFP (control; Vector Biolabs) was injected into the distal ileal lumen. Animals recovered for 2d and were then re-laparotomized and 0.75 ml oleoylethanolamide (OEA; 15 μM) was injected into the ileum followed by sampling for analysis of glycemia, plasma hormone levels and ileal gene expression, as above.

AMIC cultures were infected with 2.4x10^{7} IFU/ml Adv-iCre or Adv-RFP for 48 hr, followed by a 2 hr GLP-1 secretion assay and analysis by ELISA and qRT-PCR, as above.

Statistical Analyses Data are shown as mean ± SEM. Statistical differences were determined by Student's t test or 1- or 2-way ANOVA followed by Student's t test or Tukey multiple comparison test, as appropriate.

Results

Immunostaining of the ileum from normal mice revealed expression of syn1a in GLP-1-expressing cells, as well as in other cells in the crypt and scattered through the villous epithelium (Figure 1A). We also examined co-localization of GLP-1 and syn1a in AMIC cultures, a valuable ex vivo model for the study of GLP-1 secretion by primary L-cells (35) (Figure 1B). Importantly, of the 1.1 ± 0.1% of all AMIC cells that were GLP-1-positive (n=1670-5095 cells each in 6 independent cultures), 100% were found to co-express syn1a. Confirming specificity of the syn1a staining, AMIC cultures generated from intestinal-epithelial syn1a knockout (IE-syn1a KO) mice demonstrated a significant loss of syn1a staining in the L-cells ($p<0.001$) as well as more globally in other, unidentified crypt cells (Figure 1C-D).

GLP-1 secretion by AMIC cultures from normal mice was increased to 2.3-fold of control ($p<0.01$) in response to treatment with forskolin plus 3-isobutyl-1-methylxanthine (IBMX), without any change in GLP-1 synthesis (Figures 1E-F). Similarly, treatment with the physiological secretagogues, GIP (Figure 1G) and the GPR119 agonist, oleoylethanolamide (OEA; Figure 1H) enhanced GLP-1 release, to 1.7- and 3.5-fold of control ($p<0.05$-0.001), respectively. These findings suggest a role for syn1a in L-cell secretion and support use of both the IE-syn1a KO mouse model and AMIC cultures in further studies to assess this hypothesis.

Compared to control animals, IE-syn1a KO mice demonstrated increases in body (Figure 2A) and intestinal (Figure 2B) weight 7-12 days following the completion of daily tamoxifen injections ($p<0.05$-0.001). However, upon normalization of intestinal weight to body weight, the observed increase in intestinal weight was maintained only in male animals lacking syn1a (Figures 2C and S1), suggestive of sexual dimorphism. Morphologic characterization of the

intestinal epithelium further revealed that IE-syn1a KO animals had a small but significant increase in crypt depth ($p<0.01$; Figure 2D). Furthermore, the 39% reduction of syn1a (i.e. *Stx1a*) mRNA observed in intestinal mucosal scrapes from KO animals ($p<0.05$; Figure 2E) was associated with increases in the expression of *Stx1b* and *-2* ($p<0.05$-0.01; Figure 2F). While the function of syn1b in the intestinal epithelium is not known, it appears to play a role in mast cell degranulation (40). In contrast, *Stx2* (*aka* epimorphin) expression in mesenchymal cells abutting the epithelium has been shown to regulate the morphology of the crypt-to-villus axis (41), suggesting a role in the observed increase in crypt depth. Examination of two other syn isoforms that are also localized to the plasma membrane, *Stx3* and *-4* (42), did not reveal any other adaptive changes (Figure 2F).

To determine whether intestinal-epithelial syn1a has any relationship to glucose tolerance, we performed an oral glucose tolerance test (OGTT) in control and IE-syn1a KO mice two-days following completion of tamoxifen or vehicle injection. IE-syn1a KO animals displayed a significant impairment in glucose tolerance, with blood glucose levels reaching 1.3- and 1.4-fold of controls at t=45 ($p<0.05$) and 60 min ($p<0.001$), respectively (Figure 3A). Accordingly, the 2-hr glycemic area-under-the-curve in IE-syn1aKO mice was also significantly increased, to 1.2-fold of controls ($p<0.01$; Figure 3B). Consistent with this finding, IE-syn1a KO mice showed a reduction in plasma insulin levels as compared with controls, which reached statistical significance at t=60 min (Figure 3C). ~~Comparison of the overall glycemic response to that of insulin indicated that GSIS in IE-syn1a KO animals was reduced by 60% vs. controls ($p<0.05$; Figure 3D).~~ Furthermore, basal GLP-1 levels were 17% lower in IE-syn1a KO mice than in controls ($p<0.05$), with an even further reduction at t=10 min post-oral glucose administration (by 23%, $p<0.05$ vs. basal; $p<0.01$ vs. the difference at t=0 min; Figure 3D).

Analyzing these data for sexual dimorphism showed that male but not female IE-syn1a KO animals accounted for the glucose intolerance and reduced plasma insulin levels observed during the OGTT (Figure S2). However, plasma GLP-1 levels were consistently reduced in both male and female IE-syn1a KO animals (Figure S3A). Gene expression analysis of the GLP-1 prohormone, proglucagon (*Gcg*), in the intestinal mucosa showed no difference between KO and control animals (Figure 2F), indicating that the reduced GLP-1 levels in IE-syn1a KO mice are not due to a deficiency in GLP-1 production. Similar to the reduction in GLP-1 levels, both male and female IE-syn1a KO animals also displayed significantly lower plasma GIP concentrations, by 31 - 53% at t=0, 10 and 60 min ($p<0.05$-0.01; Figures 3E and S3B). Furthermore, a requirement for the incretin hormones in the impaired glucose tolerance of KO animals was confirmed by the demonstration that mice with loss of intestinal-epithelial syn1a had normal glucose tolerance in response to an IPGTT (Figure 3F). Together, these data suggest that the compromised glucose homeostasis in IE-syn1a KO animals occurs, at least in part, as a result of reductions in both GLP-1 and GIP secretion.

To confirm that loss of syn1a impairs L-cell secretory function, AMIC cultures were generated from crypts isolated from IE-syn1a KO and control animals. Interestingly, IE-syn1a KO AMIC cultures were found to have a 78% reduction in *Stx1a* expression ($p<0.01$; Figure 4A). This more profound knock-down in the crypt cultures compared to the mucosal scrapes is likely a consequence of epithelial cell enrichment in the cultures, whereas both villus epithelial and non-villin-expressing syn1a-positive cells contribute to the syn1a signal in the scrapes. We also examined the *Stx1b*, *-2*, *-3* and *-4* isoforms in the AMIC cultures and found no differences in expression (Figure 4B), further suggesting that adaptive changes that were observed in the mucosa were independent of the intestinal-epithelial cells.

Secretion assays with AMIC cultures generated from IE-syn1a KO mice demonstrated no difference in basal GLP-1 secretion as compared to control animals (Figure 4C). However, IE-syn1a KO mice displayed a 2.6-fold reduction in forskolin-stimulated GLP-1 secretion, to 37% of the response found in controls ($p<0.001$; Figure 4C). Total GLP-1 content of the cultured cells did not differ between the genotypes or treatment groups (Figure 4D). *Gcg* gene expression also did not differ as a result of loss of syn1a (Figure 4B), further suggesting that the reduced GLP-1 secretion is a result of disrupted L-cell secretory function.

To more directly examine the role of syn1a in GLP-1 secretion by the primary L-cell, we initially conducted in vivo and in vitro studies utilizing adenovirus-mediated knockdown of syn1a. However, application of the control adenovirus alone blunted the ability of the intestinal L-cells to respond to known secretagogues, making this an inappropriate model for further study (Figure S4). We therefore crossed the IE-syn1a KO animals with mice expressing Venus ~~YFP~~ under the control of the *Gcg* promoter (35) to permit identification of the L-cell for exocytotic analysis. While Venus-IE-syn1a KO mice did not show any changes in body weight, they were found to have increased intestinal weight which, following normalization to body weight, was maintained only in male animals lacking syn1a (Figures 5A-C and S5). This pattern was very similar to that observed in the IE-syn1a KO mice that did not express *Gcg*-Venus (Figure S1). ~~Unexpectedly, as compared to the IE-syn1a KO animals, Venus-IE-syn1a KO mice did not show any changes in body or intestinal weight, and had no evidence of sexual dimorphism (Figures 5A-C and S3).~~ Furthermore, although *Stx1a* expression was reduced by 58% ($p<0.05$) in the intestinal mucosa (Figure 5D), there were no significant changes in expression of *Stx1b* and *-2* (Figure 5E). However, an OGTT revealed that Venus-IE-syn1a KO animals, like the IE-syn1a KO mice, had impaired glucose tolerance, with significantly elevated glycemia at t=60 min after

oral glucose administration in comparison to controls (1.3-fold of control values, $p<0.05$; Figure 5F). Like the IE-syn1a KO mice, these animals also demonstrated sexual dimorphism, with significant changes found only in the male mice (Figure S6). Collectively, these findings suggested an impairment in GLP-1 secretion in the Venus-IE-syn1a KO animals, despite the finding of a 1.8-fold increase in intestinal mucosal *Gcg* gene expression ($p<0.05$; Figure 5D).

As the heterogonous cell population of both the ileal mucosa and isolated ileal crypt cultures limits our understanding of L-cell specific gene expression, we compiled a syntaxin isoform expression profile from Venus-positive L-cells by RNAseq (Figure 5G). Of the four syn isoforms known to be localized on the plasma membrane, only *Stx1a* appeared to be enriched (by 3.6-fold) in the Venus-positive L-cells as compared to Venus-negative intestinal-epithelial cells. Collectively, these data further suggest a role for syn1a in GLP-1 exocytosis, and validate the use of the Venus-IE-syn1a KO mice as a model for our studies.

As exocytosis by the primary intestinal L-cell has not previously been described, we utilized 2-photon microscopy to visualize SG fusion events in Venus-positive L-cells from both control and Venus-IE-syn1a KO mice, under basal and 50 μM forskolin-stimulated conditions (Figures 6A and S7). In the absence of forskolin, all of the Venus-positive and some of the Venus-negative cells demonstrated periodic exocytotic events; an increase in exocytosis in both cell types was noted upon the addition of forskolin. However, interestingly, some cells demonstrated a profound level of activity as compared to the surrounding cells, with a large granule size that is consistent with the known characteristics of mast cells (Supplemental Video 1) (43). As has been reported for the β-cell (24-29), distinct types of exocytotic events were observed in Venus-positive L-cells from control animals. Thus, throughout the duration of our recordings, we identified both single (full; Supplemental Video 2) and multi-granular

(compound; Supplemental Video 3) SG fusions that differed in the size of the signal and the duration of the event (Figure 6A).

The pattern of fusion events observed in L-cells from Venus-control mice was strongly indicative of biphasic exocytosis. Hence, after the basal period, the addition of forskolin stimulated a 1st-phase of exocytosis at 1-6 min, followed by a 2nd phase at 7-12 min (Figure 6B, D and E). In comparing single L-cells from Venus-IE-syn1a KO and Venus-control mice, there was no obvious change in the number of SG fusion events during the basal period (Figure 6B-E). However, recordings from Venus-IE-syn1a KO L-cells demonstrated that syn1a depletion dramatically reduced the number of SG fusion events under stimulating conditions, such that 1st phase exocytosis was reduced to basal levels ($p<0.05$) and 2nd phase was abolished ($p<0.05$). Finally, determination of the contributions of full and compound fusion events to each phase of secretion revealed that L-cell exocytosis is largely mediated by compound fusion (approximately 75% of total events), under both basal and stimulated conditions (Figure 6D). Importantly, in the absence of syn1a, the reduced number of SG fusion events in both 1st and 2nd phase secretion was attributed to the loss of both full and compound fusion. This result demonstrates the preservation of SG fusion competence under basal conditions but a requirement for syn1a in stimulated SG fusion in the primary L-cell. When taken together, these data illuminate the spatio-temporal activity of the SG exocytosis that underlies GLP-1 secretion.

Discussion

~~The incretin actions of GLP-1~~The actions of the incretin hormones, GLP-1 and GIP, account for ~50% of the insulin response to nutrient ingestion (44, 45). However, despite the importance of GLP-1 to glucose homeostasis, major gaps remain in our understanding of the molecular machinery that regulates GLP-1 release. Although studies on the primary L-cell have been limited in the past due, in large part, to the diffuse dispersion of these cells throughout the intestinal epithelium (38), recent advances now permit direct visualization of exocytosis by reporter-labelled L-cells ex vivo following primary culture (35). Using these approaches, the findings of the present study demonstrate the dynamics of SG fusion to the plasma membrane of the primary intestinal L-cell, and the essential role of the core SNARE protein, syn1a, in secretagogue-induced exocytosis of GLP-1.

2-Photon microscopy demonstrated that exocytosis by the primary L-cell is mediated through different types of exocytotic events, of which the majority are compound SG fusion rather than full fusion of single SGs, under both basal and stimulating conditions. These findings contrast to those on the β-cell, for which different types of fusion events occur during different phases of secretion (21-26, 28, 29). Hence, approximately half of 1st phase insulin secretion is mediated by predocked SGs undergoing full fusion (46). In contrast, the sustained, 2nd phase of insulin exocytosis is largely determined by influx of newcomer SGs from the intracellular reserve pool which then undergo mostly full fusion, with only a small contribution attributed to compound exocytosis (24, 28). It is important to note that the use of 2-photon microscopy in the present study precluded determination of any contribution of kiss-and-run exocytosis to GLP-1 secretion, as well as to whether the detected SGs were pre-docked or newcomer, which would be

better observed by total internal reflection fluorescence and electron microscopy. Furthermore, deletion of syn1a from the plasma membrane prevented not only single but also multi-granular fusion events. Indeed, compound fusion may require other isoforms of syn that are expressed in the L-cell (31), as demonstrated for the β-cell (23, 47). However, it is expected that prevention of initial SG fusion with the plasma membrane would preclude detection by 2-photon microscopy of any subsequent SG-to-SG interactions, including not only compound but also sequential fusion events. Thus, the factors that determine the exact nature of exocytotic fusion events in the L-cell remain to be fully defined. However, one signaling pathway that may be involved is Cdc42-dependent reorganization of the actin cytoskeleton that forms a permissive barrier to GLP-1 secretion (48) and which, therefore, may decrease the ability of SGs to move towards the plasma membrane. As a similar mechanism mediates glucose-stimulated exocytosis of newcomer SGs in the β-cell (49, 50), future studies to interrogate the relationships between Cdc42, the actin cytoskeleton and SG dynamics in the intestinal L-cell are warranted. Furthermore, altered β-cell SNARE protein expression in response to gluco- and lipotoxicity is known to affect insulin secretion (51, 52). However, although GLP-1 release is also dysregulated during feeding of a high-fat or Western diet and in association with hyperglycemia caused by circadian disruption (53-55), it currently remains unknown as to whether this is due to changes in expression of syn1a and/or other L-cell SNARE proteins.

Single-cell imaging indicated that GLP-1 secretion by the primary L-cell is biphasic, with the 1st phase occurring 1-6 min after stimulation, and a more sustained 2nd phase at 7-12 min. Interestingly, the isolated rat ileum has previously been noted to demonstrate biphasic release of GLP-1 in response to bethanechol and bombesin, but not calcitonin-gene related peptide, with a 1st peak at 2-4 min and a 2nd phase that is maintained for the duration of the vascular perfusion

(10). Furthermore, re-examination of total internal reflection fluorescence microscopy data from the GLUTag L-cell line also suggests the existence of two phases of exocytosis. Hence, ~0.4 fusions/100 μm^2-30 sec were detected under basal conditions, and this increased to ~1.5 at 1-3 min after KCl-mediated depolarization, followed by a second phase with ~1 event/100 μm^2-30 sec over the ensuing 4-7 min (31). Thus, unlike the β-cell, for which KCl-induced depolarization increases 1st phase secretion, whereas glucose induces biphasic release (21-26, 28, 29), the intestinal L-cell demonstrates biphasic secretion following activation by KCl, forskolin and some, but not all, physiological secretagogues.

As compared to the normal intestine, wherein L-cells constitute ~0.5% of epithelial cells (56), 1.1% of the cells in the AMIC cultures were found to express GLP-1, indicating a relative enrichment in this ileal crypt-cell model. Furthermore, 100% of the AMIC L-cells were found to express syn1a and, of the syntaxin isoforms known to be expressed on the plasma membrane (*Stx1a*, *-1b*, *-2*, *-3, -4*; (42)), only *Stx1a* was found to be enriched. Consistent with an ~~essential~~ important role for this core SNARE protein in the L-cell, KO of syn1a reduced forskolin-stimulated GLP-1 secretion at both the single-cell and population level in AMIC cultures, and reduced OGTT-induced GLP-1 release in the mouse in vivo. While no profound effects of the KO were found on basal GLP-1 release in the ex vivo and single-cell models examined, basal GLP-1 levels were reduced in vivo as a potential consequence of villin-driven cre expression, resulting in altered release of or responsiveness to paracrine regulators of GLP-1 secretion. Of note, IE-syn1a KO animals demonstrated even greater reductions in basal- and stimulated GIP secretion, likely contributing to the glucose intolerant phenotype through both the reduction of its own insulinotropic actions and via reduced L-cell stimulation by GIP (11). Future studies examining exocytotic dynamics in the GIP-producing K-cell are clearly warranted. ~~majority of~~

~~the models examined, possible roles for other syntaxin isoforms in the L-cell cannot be discounted.~~ Finally, the maintenance of basal L-cell exocytosis and only partial loss of 1st phase of secretion in the absence of syn1a could suggest contributions by another syn isoform in the L-cell to mediate fusion of pre-docked SGs, with the almost complete loss of 2nd phase secretion explained by the loss of syn1a-mediated newcomer SG fusion, comparable to findings in the β-cell (47). Nonetheless, our previous report of expression of VAMP2 in primary L-cells, a role for VAMP2 in GLP-1 release, and an interaction between VAMP2, syn1a and SNAP25 in the GLUTag cells (31) is consistent with the notion that these proteins form a core SNARE complex in the primary intestinal L-cell.

Although both of the syn1a KO models used in this study were generated from villin-creER$^{T2+/0}$ and syn1a$^{fl/fl}$ mice, small differences were noted in the IE-syn1a KO mice as compared those crossed with the *Gcg*-Venus animals. Hence, the IE-syn1a KO mice demonstrated ~~sexually dimorphic increases in body and intestinal weight, slightly deeper crypts and~~increases in *Stx1b* and *Stx2* expression. Conversely, the Venus-IE-syn1a KO exhibited an increase only in *Gcg* expression, which could reflect a potential effect of proglucagon-driven Venus expression in the L-cell. However, the subtle differences in gene expression between the KO models was presumed not to influence GLP-1 secretion, as L-cell secretion was found to be impaired by loss of syn1a in both the ex vivo secretion assays (IE-syn1a KO) and single-cell experiments (Venus-IE-syn1a KO). Furthermore, when taken with the rigorous inclusion of multiple genotypes as controls for each of these animal models, our finding of consistent effects of syn1a KO to reduce GLP-1 secretion suggests that these small differences in the mouse models had no impact on the conclusions of this study.

Interestingly, while both male and female animals displayed significantly reduced GLP-1 and GIP levels, IE-syn1a KO mice demonstrated sexual dimorphism in their metabolic responses to oral glucose administration; similar differences in glucose tolerance were also found in the Venus-IE-syn1a KO animals. The female animals therefore demonstrated an improved capacity to compensate for the reduction in the incretin hormones. However, whether these findings can be extrapolated to humans remains unclear, as a previous study has indicated that OGTT-induced changes in the levels of glucose, insulin and both of the incretin hormones are all increased in women (57).

The mechanisms underlying GLP-1 release from the intestinal L-cell are of increasing interest as a therapeutic approach to the treatment of hyperglycemia in patients with T2D, either alone or in combination with DPP IV inhibition (5-7). Our findings identify an exquisite mechanism of metered secretory output that precisely regulates release of the incretin, GLP-1 and, hence, insulin secretion following a meal. Furthermore, as the intestinal L-cell co-secretes a number of other biologically active peptide hormones, these findings may also have implications in other disease states. The demonstration of a role for syn1a in modulating stimulated SG fusion events provides impetus for further studies to elucidate the full complement of SNARE and cognate accessory proteins in the primary L-cell that mediate distinct exocytotic events, as well as their coupling to the diverse signaling pathways that are activated by nutrient ingestion. Elucidation of the exact mechanisms underlying GLP-1 release holds important implications for development of GLP-1 secretagogues to treat patients with T2D or obesity.

Author Contributions

SEW, HMS, YN, SJH, ABH, FR, FMG and PL researched data. SEW and PLB wrote the manuscript. HMS, YN, SJH, ABH, FR, FMG and HYG reviewed/edited the manuscript.

Acknowledgements

SEW and HMS were supported by Ontario Graduate Scholarships; SEW by Novo-Nordisk Banting and Best Diabetes Centre (BBDC, University of Toronto) Graduate Studentships; YN by a University of Toronto Research Opportunity Summer Studentship; SJH by a BBDC Summer Studentship; and PLB by the Canada Research Chairs program. These studies were supported by an operating grant to PLB from the Natural Sciences and Engineering Research Council of Canada (RGPIN418). The Nikon A1R multi-photon microscope and the Mesoscale Discovery Sector 2400A used in this study was supported by The 3D (Diet, Digestive Tract and Disease) Centre funded by the Canadian Foundation for Innovation and Ontario Research Fund, project number 19442 and 30961. Research in the Reimann/Gribble laboratory was funded by the Wellcome Trust (106262/Z/14/Z, 106263/Z/14/Z) and the Medical Research Council (MRC_MC_UU_12012/3, MRC_MC_UU_12012/5).

Duality of Interest

The authors have no conflicts of interest to report.

Guarantor

PLB takes full responsibility for the content of this manuscript.

References

1. Campbell JE, Drucker DJ. Pharmacology, physiology, and mechanisms of incretin hormone action. *Cell Metab*. 2013;**17**:819-837

2. Dong CX, Brubaker PL. Ghrelin, the proglucagon-derived peptides and peptide YY in nutrient homeostasis. *Nat. Rev. Gastroenterol. Hepatol*. 2012;**9**:705-715

3. Mulvihill EE, Drucker DJ. Pharmacology, physiology, and mechanisms of action of dipeptidyl peptidase-4 inhibitors. *Endocr Rev*. 2014;**35**:992-1019

4. Nauck M. Incretin therapies: highlighting common features and differences in the modes of action of glucagon-like peptide-1 receptor agonists and dipeptidyl peptidase-4 inhibitors. *Diabetes Obes Metab*. 2016;**18**:203-216

5. Brubaker PL. Minireview: Update on incretin biology: focus on glucagon-like peptide-1. *Endocrinology*. 2010;**151**:1984-1989

6. Drucker DJ. Evolving concepts and translational relevance of enteroendocrine cell biology. *J Clin Endocrinol Metab*. 2016;**101**:778-786

7. Pais R, Gribble FM, Reimann F. Stimulation of incretin secreting cells. *Ther Adv Endocrinol Metab*. 2016;**7**:24-42

8. Carr RD, Larsen MO, Jelic K, Lindgren O, Vikman J, Holst JJ, Deacon CF, Ahren B. Secretion and dipeptidyl peptidase-4-mediated metabolism of incretin hormones after a mixed meal or glucose ingestion in obese compared to lean, nondiabetic men. *J. Clin. Endocrinol. Metab*. 2010;**95**:872-878

9. Moller JB, Jusko WJ, Gao W, Hansen T, Pedersen O, Holst JJ, Overgaard RV, Madsen H, Ingwersen SH. Mechanism-based population modelling for assessment of L-cell function based on total GLP-1 response following an oral glucose tolerance test. *J. Pharmacokinet. Pharmacodyn*. 2011;**38**:713-725

10. Dumoulin V, Dakka T, Plaisancie P, Chayvialle J-A, Cuber J-C. Regulation of glucagon-like peptide-1-(7-36)amide, peptide YY, and neurotensin secretion by neurotransmitters and gut hormones in the isolated vascularly perfused rat ileum. *Endocrinology*. 1995;**136**:5182-5188

11. Rocca AS, Brubaker PL. Role of the vagus nerve in mediating proximal nutrient-induced glucagon-like peptide-1 secretion. *Endocrinology*. 1999;**140**:1687-1694

12. Anini Y, Hansotia T, Brubaker PL. Muscarinic receptors control postprandial release of glucagon-like peptide-1: In vivo and in vitro studies in rats. *Endocrinology*. 2002;**143**:2420-2426

13. Parker HE, Adriaenssens A, Rogers G, Richards P, Koepsell H, Reimann F, Gribble FM. Predominant role of active versus facilitative glucose transport for glucagon-like peptide-1 secretion. *Diabetologia*. 2012;**55**:2445-2455

14. Lauffer LM, Iakoubov R, Brubaker PL. GPR119 is essential for oleoylethanolamide-induced glucagon-like peptide-1 secretion from the intestinal enteroendocrine L-cell. *Diabetes*. 2009;**58**:1058-1066

15. Tolhurst G, Heffron H, Lam YS, Parker HE, Habib AM, Diakogiannaki E, Cameron J, Grosse J, Reimann F, Gribble FM. Short-chain fatty acids stimulate glucagon-like peptide-1 secretion via the G-protein-coupled receptor FFAR2. *Diabetes*. 2012;**61**:364-371

16. Habib AM, Richards P, Rogers GJ, Reimann F, Gribble FM. Co-localisation and secretion of glucagon-like peptide 1 and peptide YY from primary cultured human L cells. *Diabetologia*. 2013;**56**:1413-1416

17. Li J, Klughammer J, Farlik M, Penz T, Spittler A, Barbieux C, Berishvili E, Bock C, Kubicek S. Single-cell transcriptomes reveal characteristic features of human pancreatic islet cell types. *EMBO Rep*. 2016;**17**:178-187

18. Rutter GA, Pullen TJ, Hodson DJ, Martinez-Sanchez A. Pancreatic beta-cell identity, glucose sensing and the control of insulin secretion. *Biochem J*. 2015;**466**:203-218

19. Dolai S, Xie L, Zhu D, Liang T, Qin T, Xie H, Kang Y, Chapman ER, Gaisano HY. Synaptotagmin-7 functions to replenish insulin granules for exocytosis in human islet beta-cells. *Diabetes*. 2016;**65**:1962-1976

20. Sudhof TC, Rothman JE. Membrane fusion: grappling with SNARE and SM proteins. *Science*. 2009;**323**:474-477

21. Oh E, Kalwat MA, Kim MJ, Verhage M, Thurmond DC. Munc18-1 regulates first-phase insulin release by promoting granule docking to multiple syntaxin isoforms. *J. Biol. Chem*. 2012;**287**:25821-25833

22. Takahashi N, Hatakeyama H, Okado H, Noguchi J, Ohno M, Kasai H. SNARE conformational changes that prepare vesicles for exocytosis. *Cell Metab*. 2010;**12**:19-29

23. Xie L, Zhu D, Dolai S, Liang T, Qin T, Kang Y, Xie H, Huang YC, Gaisano HY. Syntaxin-4 mediates exocytosis of pre-docked and newcomer insulin granules underlying biphasic glucose-stimulated insulin secretion in human pancreatic beta cells. *Diabetologia*. 2015;**58**:1250-1259

24. Gaisano HY. Here come the newcomer granules, better late than never. *Trends Endocrinol Metab*. 2014;**25**:381-388

25. Takahashi N, Hatakeyama H, Okado H, Miwa A, Kishimoto T, Kojima T, Abe T, Kasai H. Sequential exocytosis of insulin granules is associated with redistribution of SNAP25. *J Cell Biol*. 2004;**165**:255-262

26. Hoppa MB, Jones E, Karanauskaite J, Ramracheya R, Braun M, Collins SC, Zhang Q, Clark A, Eliasson L, Genoud C, Macdonald PE, Monteith AG, Barg S, Galvanovskis J, Rorsman P. Multivesicular exocytosis in rat pancreatic beta cells. *Diabetologia*. 2012;**55**:1001-1012

27. Hanna ST, Pigeau GM, Galvanovskis J, Clark A, Rorsman P, MacDonald PE. Kiss-and-run exocytosis and fusion pores of secretory vesicles in human beta-cells. *Pflugers Arch*. 2009;**457**:1343-1350

28. Gaisano HY. Deploying insulin granule-granule fusion to rescue deficient insulin secretion in diabetes. *Diabetologia*. 2012;**55**:877-880

29. Wang Z, Thurmond DC. Mechanisms of biphasic insulin-granule exocytosis - roles of the cytoskeleton, small GTPases and SNARE proteins. *J. Cell Sci*. 2009;**122**:893-903

30. Gustavsson N, Wang Y, Kang Y, Seah T, Chua S, Radda GK, Han W. Synaptotagmin-7 as a positive regulator of glucose-induced glucagon-like peptide-1 secretion in mice. *Diabetologia*. 2011;**54**:1824-1830

31. Li SK, Zhu D, Gaisano HY, Brubaker PL. Role of vesicle-associated membrane protein 2 in exocytosis of glucagon-like peptide-1 from the murine intestinal L cell. *Diabetologia*. 2014;**57**:809-818

32. Liang T, Qin T, Xie L, Dolai S, Zhu D, Prentice KJ, Wheeler MB, Kang Y, Osborne L, Gaisano HY. New roles of syntaxin-1A in insulin granule exocytosis and replenishment. *J. Biol. Chem.* 2017;**292**:2203-2216

33. el Marjou F, Janssen KP, Chang BH, Li M, Hindie V, Chan L, Louvard D, Chambon P, Metzger D, Robine S. Tissue-specific and inducible Cre-mediated recombination in the gut epithelium. *Genesis*. 2004;**39**:186-193

34. Rowland KJ, Trivedi S, Wan K, Kulkarni RN, Holzenberger M, Robine S, Brubaker PL. Loss of glucagon-like peptide-2-induced proliferation following intestinal epithelial insulin-like growth factor-1 receptor deletion. *Gastroenterology*. 2011;**141**:2166-2175

35. Reimann F, Habib AM, Tolhurst G, Parker HE, Rogers GJ, Gribble FM. Glucose sensing in L cells: a primary cell study. *Cell Metab*. 2008;**8**:532-539

36. Lim GE, Huang GJ, Flora N, LeRoith D, Rhodes CJ, Brubaker PL. Insulin regulates glucagon-like peptide-1 secretion from the enteroendocrine L cell. *Endocrinology*. 2009;**150**:580-591

37. Gagnon J, Baggio LL, Drucker DJ, Brubaker PL. Ghrelin is a novel regulator of GLP-1 secretion. *Diabetes*. 2015;**64**:1513-1521

38. Eissele R, Göke R, Willemer S, Harthus HP, Vermeer H, Arnold R, Göke B. Glucagon-like peptide-1 cells in the gastrointestinal tract and pancreas of rat, pig and man. *Eur. J. Clin. Invest*. 1992;**22**:283-291

39. Schneider CA, Rasband WS, Eliceiri KW. NIH Image to ImageJ: 25 years of image analysis. *Nat Methods*. 2012;**9**:671-675

40. Sander LE, Frank SP, Bolat S, Blank U, Galli T, Bigalke H, Bischoff SC, Lorentz A. Vesicle associated membrane protein (VAMP)-7 and VAMP-8, but not VAMP-2 or VAMP-3, are required for activation-induced degranulation of mature human mast cells. *Eur J Immunol*. 2008;**38**:855-863

41. Fritsch C, Swietlicki EA, Lefebvre O, Kedinger M, Iordanov H, Levin MS, Rubin DC. Epimorphin expression in intestinal myofibroblasts induces epithelial morphogenesis. *J Clin Invest*. 2002;**110**:1629-1641

42. Wheeler MB, Sheu L, Ghai M, Bouquillon A, Grondin G, Weller U, Beaudoin AR, Bennett MK, Trimble WS, Gaisano HY. Characterization of SNARE protein expression in β cell lines and pancreatic islets. *Endocrinology*. 1996;**137**:1340-1348

43. Horiguchi K, Yoshikawa S, Saito A, Haddad S, Ohta T, Miyake K, Yamanishi Y, Karasuyama H. Real-time imaging of mast cell degranulation in vitro and in vivo. *Biochem Biophys Res Commun*. 2016;**479**:517-522

44. Nauck MA, Homberger E, Siegel EG, Allen RC, Eaton RP, Ebert R, Creutzfeldt W. Incretin effects of increasing glucose loads in man calculated from venous insulin and C-peptide responses. *J. Clin. Endocrinol. Metab*. 1986;**63**:492-498

45. Wang Z, Wang RM, Owji AA, Smith DM, Ghatei MA, Bloom SR. Glucagon-like peptide-1 is a physiological incretin in rat. *J. Clin. Invest*. 1995;**95**:417-421

46. Ohara-Imaizumi M, Fujiwara T, Nakamichi Y, Okamura T, Akimoto Y, Kawai J, Matsushima S, Kawakami H, Watanabe T, Akagawa K, Nagamatsu S. Imaging analysis reveals mechanistic differences between first- and second-phase insulin exocytosis. *J. Cell Biol*. 2007;**177**:695-705

47. Zhu D, Koo E, Kwan E, Kang Y, Park S, Xie H, Sugita S, Gaisano HY. Syntaxin-3 regulates newcomer insulin granule exocytosis and compound fusion in pancreatic beta cells. *Diabetologia*. 2013;**56**:359-369

48. Lim GE, Xu M, Sun J, Jin T, Brubaker PL. The Rho guanosine 5'-triphosphatase, Cell Division Cycle 42, is required for insulin-induced actin remodeling and glucagon-like peptide-1 secretion in the intestinal endocrine L cell. *Endocrinology*. 2009;**150**:5249-5261

49. Nevins AK, Thurmond DC. Glucose regulates the cortical actin network through modulation of Cdc42 cycling to stimulate insulin secretion. *Am. J. Physiol Cell Physiol*. 2003;**285**:C698-C710

50. Lam PP, Ohno M, Dolai S, He Y, Qin T, Liang T, Zhu D, Kang Y, Liu Y, Kauppi M, Xie L, Wan WC, Bin NR, Sugita S, Olkkonen VM, Takahashi N, Kasai H, Gaisano HY. Munc18b is a major mediator of insulin exocytosis in rat pancreatic beta-cells. *Diabetes*. 2013;**62**:2416-2428

51. Gaisano HY, Ostenson CG, Sheu L, Wheeler MB, Efendic S. Abnormal expression of pancreatic islet exocytotic soluble N-ethylmaleimide-sensitive factor attachment protein receptors in Goto-Kakizaki rats is partially restored by phlorizin treatment and accentuated by high glucose treatment. *Endocrinology*. 2002;**143**:4218-4226

52. Ostenson CG, Chen J, Sheu L, Gaisano HY. Effects of palmitate on insulin secretion and exocytotic proteins in islets of diabetic Goto-Kakizaki rats. *Pancreas*. 2007;**34**:359-363

53. Gil-Lozano M, Mingomataj EL, Wu WK, Ridout SA, Brubaker PL. Circadian secretion of the intestinal hormone GLP-1 by the rodent L cell. *Diabetes*. 2014;**63**:3674-3685

54. Gil-Lozano M, Wu WK, Martchenko A, Brubaker PL. High fat diet and palmitate alter the time-dependent secretion of glucagon-like peptide-1 by the rodent L-cell. *Endocrinology*. 2016;**157**:586-599

55. Richards P, Pais R, Habib AM, Brighton CA, Yeo GS, Reimann F, Gribble FM. High fat diet impairs the function of glucagon-like peptide-1 producing L-cells. *Peptides*. 2016;**77**:21-27

56. Petersen N, Reimann F, Bartfeld S, Farin HF, Ringnalda FC, Vries RG, van den Brink S, Clevers H, Gribble FM, de Koning EJ. Generation of L cells in mouse and human small intestine organoids. *Diabetes*. 2014;**63**:410-420

57. Vaag AA, Holst JJ, Volund A, Beck-Nielsen H. Gut incretin hormones in identical twins discordant for non-insulin-dependent diabetes mellitus (NIDDM) - Evidence for decreased glucagon-like peptide 1 secretion during oral glucose ingestion in NIDDM twins. *Eur. J. Endocrinol*. 1996;**135**:425-432

Figure Legends

Figure 1: Primary murine intestinal L-cells express syn1a and secrete GLP-1 in vitro. (**A-D**) Mouse intestine (**A**) and AMIC cultures (**B-C**) were immunostained for GLP-1 (red) and syn1a (green); DAPI is blue, negative controls are shown in the inset, and arrows indicate GLP-1-positive cells. Representative images are shown from n=6 IE-syn1a control (**A-B**) mice, and from n=4 IE-syn1a KO animals (**C**). Quantification of control and IE-syn1a KO AMIC L-cell syntaxin-1a immunofluorescence intensity (**D**; n=4 cells from 4 control mice and n=6 cells from 5 IE-syn1a KO mice). (**E-H**) AMIC cultures from C57Bl/6 mice were treated for 2hr with forskolin/IBMX (**E-F**; n=10-11), or varying concentrations of GIP (**G**; n=7-12) or OEA (**H**; n=5-7) with forskolin as the positive control. GLP-1 secretion as a percent of total content and total GLP-1 content for the same cultures are shown in (**E-F**), respectively. * $p<0.05$, ** $p<0.01$ and *** $p<0.001$ vs. vehicle control.

Figure 2: IE-syn1a KO mice demonstrate small intestinal adaptive responses. (**A-C**) Body weight (**A**), small intestinal weight (**B**), and small intestinal weight normalized to body weight (**C**) in male and female control and IE-syn1a KO mice (n= 10-13). (**D**) ~~Crypt-~~Crypt depth and villus height in control and IE-syn1a KO mice (n=5-8). (**E-F**) *Stx1a* (**E**) and *Stx* isoform and *Gcg* (**F**) transcript levels in ileal mucosal scrapes from control and IE-syn1a-KO mice (n=10-13). * $p<0.05$, ** $p<0.01$ and *** $p<0.001$ vs. control mice.

Figure 3: IE-syn1a KO mice demonstrate reduced GLP-1 secretory responses during an OGTT in association with impaired glucose tolerance. (**A-E**) Male and female control and IE-syn1a KO mice (n=8-22) were administered an OGTT at t=0 min followed by blood sampling at 0, 10, 60,

90 and 120 min; a second cohort of mice (n=7-10) also included sampling for blood glucose at t = 30 and 45 min. ~~for determination of~~ Blood glucose (**A**), glycemic area-under-the-curve (AUC, **B**) and plasma insulin (**C**), ~~the ratio of the glucose to insulin response~~ GLP-1 (**D**; plasma GLP-1 levels were normalized to control levels at t=0 min (20.8 ± 3.1 pg/ml; n=25) to account for variance found between two different assay plates) and GIP (**E**). ~~and plasma GLP-1 levels (E).~~ (**F**) Separate cohorts of male and female mice (n=6) were administered an IPGTT at t=0 min followed by blood sampling for determination of blood glucose. * p<0.05, ** p<0.01 and *** p<0.001 vs. control mice or as indicated for the delta response.

Figure 4: AMIC cultures from IE-syn1a KO mice demonstrate reduced GLP-1 secretory responses. (**A-B**) *Stx1a* (**A**) and *Stx* isoform and *Gcg* (**B**) transcript levels in AMIC cultures from male and female control and IE-syn1a KO mice (n=4-6). (**C-D**) Control and IE-syn1a KO AMIC cultures were treated for 2 hr with vehicle (basal) or forskolin plus IBMX (n=7-9), followed by determination of GLP-1 release into the media (**C**; control basal secretion was 5.9 ± 2.2% of total cell content) and (**D**) GLP-1 content in the media plus cells. ** p<0.01 and *** p<0.001 vs. basal; ### p<0.001 vs. same treatment in controls.

Figure 5: Venus-IE-syn1a KO mice demonstrate impaired glucose tolerance during an OGTT. (**A-C**) Body weight (**A**), small intestinal weight (**B**) and small intestinal weight normalized to body weight (**C**) in male and female control and IE-syn1a-KO mice. (**D-E**) mRNA transcript levels for *Stx1a* (**D**) and *Stx* isoforms and *Gcg* (**E**) in ileal mucosal scrapes from control and IE-syn1a-KO mice. (**F**) Control and IE-syn1a KO mice were administered an OGTT at t=0 min followed by blood sampling for determination of blood glucose levels (n=9-12 for **A-F**). (**G)**

RNAseq for syntaxin isoforms in FACS-isolated Venus^{+} vs. Venus^{-} jejunal/ileal epithelial cells from female *Gcg*-Venus mice (inset shows expanded scale; n=3). FPKM, fragments per kilobase of exon per million fragments mapped.

Figure 6: 2-Photon microscopy of primary ileal L-cells demonstrates the role of syn1a in multiple forms of exocytosis. (**A**) Representative images and fluorescent intensity tracings of single/full SG and multi-granular/compound SG fusion events in Venus-positive L-cells from control mice. (**B-E**) Quantification of the total number of fusion events collected over a 3 min basal period and a 12 min forskolin infusion period in control (**B**) and Venus-IE-syn1a KO (**C**) mice; (**D**) indicates the same data binned into different phases of secretion (basal: t = -3 to -1 min; 1st phase: t = 1 to 6 min; and 2nd phase: t = 7 to 12 min) and then classified as full vs. compound fusion. The dotted line in (**B**) indicates best-fit curve for stimulated exocytosis (R^2 = 0.82). *p<0.05, ** p<0.01 and *** p<0.001 vs. basal; # p<0.05 and ### p<0.001 vs. the same phase in control mice, for total fusion events. (**E**) Cumulative total fusion events. * p<0.05, ** p<0.01 for each time point at t = 4-12 min. n= 9 cells from 6 control mice and 6 cells from 3 IE-Venus-syn1a KO.

SUPPLEMENTAL MATERIALS

Supplemental Figure Legends

Figure S1: Body weight (**A**), intestinal weight (**B**) and intestinal weight normalized to body weight (**C**) in the male vs. female control and IE-syn1a KO mice shown in Figure 2.

Figure S2: Blood glucose (**A**), and plasma insulin (**B**) levels in the male vs. female control and IE-syn1a KO mice shown in Figure 3.

Figure S3: Plasma GLP-1 (**A**), and GIP (**B**) levels in the male vs. female control and IE-syn1a KO mice shown in Figure 3.

Figure S4: (**A-B**) Male C57Bl/6 mice were administered ileal AdV-RFP (control) or AdV-iCre followed by intra-ileal administration of OEA 2 d later, and determination of mucosal *Stx1a* mRNA transcript levels (**A**) and plasma GLP-1 levels (**B**; n=3-4). (**C-D**) AMIC cultures from male C57Bl/6 mice were treated with AdV-RFP (control) or AdV-iCre for 2 d, followed by 2 hr treatment with vehicle (basal), forskolin plus IBMX or OEA for 2 hr, and determination of cell *Stx1a* mRNA transcript levels (**C**) and GLP-1 content in the media and cells (**D**; n=4).

Figure S5: Body weight (**A**), intestinal weight (**B**) and intestinal weight normalized to body weight (**C**) in the male vs. female control and Venus-IE-syn1a-KO mice shown in Figure 5.

Figure S6: Blood glucose levels in the male vs. female control and Venus-IE-syn1a KO mice shown in Figure 5.

Figure S7: Representative 2-photon images of full and compound fusion events using SRB (red) and Venus (green), as visualized in the respective cells shown in Figure 6A.

Supplemental Video 1: Full-field view of a Venus$^+$ L-cell (green) surrounded by unlabelled cells. Forskolin was added at t = 30 sec. Note the large granule size and multiple fusion events occurring in a single neighbouring cell (arrow), consistent with the known properties of mast cells. The same video is submitted in both .avi and .mp4 format.

Supplemental Video 2: Single granule, full fusion event at t = 577.8 sec in the membrane of a Venus$^+$ L-cell. The same video is submitted in both .avi and .mp4 format.

Supplemental Video 3: Multi-granular, compound fusion event at t = 129.3 – 255.3 sec in the membrane of a Venus$^+$ L-cell. The same video is submitted in both .avi and .mp4 format.

Table S1: Genotyping primers

Gene	Forward	Reverse	Amplicon (bp)	Annealing Temperature (^{O}C)
Stx1a	GCT GCA GAA GCA AGA GAA CC	CAG CCA TAC AAA AAC CAC CA	WT: 404 Flox: 239	50.0
Cre	CAA GCC TGG CTC GAC GGC C	CGC GAA CAT CTT CAG GTT CT	390	50.0
Gcg/GFP	AAT TGA GCT CAT TTG GAC TGC C	CTT GCC GTA GGT GGC ATC G	210	50.0
GFP/GFP	CTG GTA GTG GTC GGC GAG C	GTT CAG CGT GTC CGG CGA G	470	50.0

Table S2: Antibody table

Sample	Antigen	Primary Antiserum	Secondary Antiserum
Ileal Tissue	Syntaxin1a	Rabbit anti-syn1a, 1:500 (Abcam cat#41453)	AlexaFluor488-goat anti-rabbit IgG, 1:150 (Life Technologies)
	GLP-1	Mouse anti-GLP-1, 1:400 (Abcam cat # 23472)	AlexaFluro555-goat anti-mouse IgG, 1:150 (Life Technologies)
AMIC Culture	Syntaxin1a	Rabbit anti-syn1a, 1:1000 (Abcam cat#41453)	AlexaFluor488-goat anti-rabbit IgG, 1:150 (Life Technologies)
	GLP-1	Mouse anti-GLP-1, 1:200 (Abcam cat # 23472)	AlexaFluro555-goat anti-mouse IgG, 1:150 (Life Technologies)

Table S3: qRT-PCR Primer/Probes (all from Applied Biosystems)

Transcript	Product number	Exons targeted
Gcg	Mm00801714_m1	5-6
H3f3a	Mm01612808_g1	3-4
Stx1a	Mm00444008_m1	1-2
Stx1b	Mm01275274_m1	1-2
Stx2	Mm04229900_m1	2-3
Stx3	Mm01197689_m1	6-7
Stx4	Mm00436827_m1	5-6